

# NATIONAL INSTITUTE FOR FUSION SCIENCE

## Cross Section Database for Collision Processes of Helium Atom with Charged Particles. I. Electron Impact Processes.

Yu. V. Ralchenko, R. K. Janev, T. Kato, D.V. Fursa, I. Bray and F.J. de Heer

(Received - Oct. 2, 2000 )

NIFS-DATA-59

Oct. 2000

This report was prepared as a preprint of compilation of evaluated atomic, molecular, plasma-wall interaction, or nuclear data for fusion research, performed as a collaboration research of the Data and Planning Center, the National Institute for Fusion Science (NIFS) of Japan. This document is intended for future publication in a journal or data book after some rearrangements of its contents.

Inquiries about copyright and reproduction should be addressed to the Research Information Center, National Institute for Fusion Science, Oroschi, Toki, Gifu, 509-5292, Japan.

## RESEARCH REPORT NIFS-DATA Series

TOKI, JAPAN

# Cross section database for collision processes of helium atom with charged particles. I. Electron impact processes.

Yu. V. Ralchenko<sup>\*†</sup>, R. K. Janev<sup>\*‡</sup>, T. Kato\*,  
D. V. Fursa<sup>§</sup>, I. Bray<sup>§</sup> and F. J. de Heer<sup>¶</sup>

Received October 23, 2000

## Abstract

A comprehensive and critically assessed cross section database for the inelastic collision processes of ground state and excited helium atoms colliding with electrons, protons and multiply-charged ions has been prepared at the Data and Planning Center at NIFS. The present report describes the first part of the database containing the recommended data for electron impact excitation and ionization of neutral helium. All states (atomic terms) with  $n \leq 4$  are treated individually while the states with  $n > 4$  are considered degenerate. For the processes involving transitions to and from  $n > 4$  levels, suitable cross section scaling relations are presented. For a large number of electron impact transitions, both from the ground and excited states, new convergent close coupling (CCC) calculations were performed to achieve a high accuracy of the data. The evaluated/recommended cross section data are presented by analytic fit functions which preserve the correct asymptotic behavior of the cross sections. The cross sections are also displayed in a graphical form.

**Key words:** atomic database – electron impact excitation – electron impact ionization – neutral helium

---

\*National Institute for Fusion Science, Oroshi-cho, Toki-shi, Gifu-ken 509-52, Japan

†Faculty of Physics, Weizmann Institute of Science, Rehovot 76100, Israel

‡Macedonian Academy of Sciences and Arts, P.O.Box 482, 91000 Skopje, Macedonia

§Flinder University, Adelaide, Australia

¶FOM Institute for Atomic and Molecular Physics, Amsterdam, The Netherlands

# 1 Introduction

The collisional processes of helium atoms with electrons and atomic ions are of interest in many research fields. The assembling of the present database for the collisional processes of helium atoms with electrons, protons and multiply charged ions, however, has been largely motivated by the urgent needs for such a database in fusion energy research. Neutral helium beams injected into the plasma of a fusion device can be used either for diagnostic purposes [1, 2] or for plasma heating [3]. The penetration of energetic neutral beams in fusion plasmas is affected by all inelastic collision processes of beam atoms with plasma electrons, protons and impurity ions [4]. Multistep processes, such as excitation followed by ionization or electron capture, can significantly enhance the beam attenuation and, therefore, the beam attenuation calculations require knowledge of the cross sections for collisional processes (in principle) for all (ground and excited) states of the helium atom with plasma constituents. This knowledge is also required to determine the populations of different excited states in the beam emission plasma diagnostics [5] or in other plasma experiments [6].

There exists a significant amount of cross section information for all inelastic collision processes of He in its ground state with electrons, protons and multiply charged atomic ions. This information has been a subject of collection and critical assessment in several publications in the past [7, 8, 9, 10, 11, 12, 13]. The cross section data for the collision processes involving excited helium atoms have started to become available only recently, and mainly for the electron impact processes (see, e.g., [13, 14, 15]).

The purpose of the present report is to critically reassess the available data information for the collision processes of ground state and excited helium atoms with electrons and to present new cross section data for the electron-impact induced transitions between the states with  $1s \leq nl \leq 4f$  and from these states to the continuum. The heavy-particle impact processes will be presented in a separate publication thereby completing a comprehensive and critically evaluated cross section database for neutral helium.

The one- and two-electron collision processes for

which cross section data are included in the present database are electron impact excitation and single and double ionization. The strategy which we adopt in presenting the data and in constructing the database is as follows. Having in mind various types of potential applications of this database (plasma diagnostics, neutral beam attenuation modeling, etc.), we treat the states with  $n \leq 4$  as individual ( $l$ -resolved) atomic terms while the states with  $n \geq 5$  are considered (generally) as degenerate. For the excitation transitions from the  $n \leq 4$  group of states to the  $n \geq 5$  group of states (levels), as well as for the transitions between the states with  $n \geq 5$ , we use scaling relationships with demonstrated applicability. The cross sections for ionization transitions from the higher  $n$ -states with  $n \geq 5$  are also described by such scaling relations. The extensive use of cross section scaling relationships in this work has been motivated by the need to provide a complete collisional database for self-consistent calculations of the population kinetics of He states in a fusion plasma.

The primary source for the cross sections for electron-impact excitation of singlet and triplet states up to  $n = 3 - 6$  (depending on the value of total angular momentum  $L$ ) were Refs. [12] and [16]. For the transitions between the states with  $2 \leq n \leq 4$  (but also including some transitions from the ground state to correct the data of Ref. [12]), we have performed new cross section calculations with the convergent close coupling (CCC) method [17] by employing 89 coupled states. This method (and basis set) was used also to calculate the ionization cross sections for the  $n \leq 4$  states (except for the ionization from the ground and  $1s2s\ 3S$  states for which experimental data were used, see e.g. Ref. [18]).

The scaling relations used to generate electron impact excitation or ionization cross sections for the  $n \leq 5$  states were based mainly on the Born approximation (for dipole allowed transitions) or classical mechanics arguments [19]. We should note, however, that the cross section scaling relations were applied in the majority of cases for transitions to, between, and from high- $n$  states, the populations of which are mostly determined by collisional rather than radiative processes and thus do not strongly depend on the accuracy of the atomic data involved. Therefore,

the uncertainties associated with the application of some of the cross section scaling relationships do not compromise the accuracy of the database from the point of view of its practical applications.

The cross sections considered as presently the best available ("recommended"), obtained by critical assessment of the available experimental and theoretical data (including the recommended cross section data contained in Refs. [11] and [12]) or by the accurate CCC 89-states calculations of the present work (for electron impact excitation and ionization of  $1 \leq n \leq 4$  states), have been fitted to analytic expressions which ensure correct asymptotic behavior of the cross sections. The recommended cross sections for the specific processes are represented both by their analytic fit function, together with the associated fitting coefficients, and in graphical form. Detailed description of data presentation is given in the next section, followed by the tables of fitting coefficients and the graphs of the cross sections.

## 2 Electron impact excitation

We shall be generally designating the electronic states (terms) of He in an abbreviate form by indicating in the state notation only the principal quantum number  $n$  of the "active" electron, the total electron angular momentum  $L$ , and the spin multiplicity  $2S+1$ , where  $S$  is the total electron spin. Thus, the excited state  $1s n l\ 2S+1 L$  will be designated as  $n^{2S+1} L$ . (Doubly excited states are not considered in the present work.) For example, the transition from the ground state to an excited state is therefore designated as  $1^1 S \rightarrow n^{2S+1} L$ , with  $2S+1 = 1$  or 3.

As mentioned in the Introduction, a very detailed critical assessment of the electron-impact excitation cross sections for the transitions  $1^1 S - n^{1,3} L$  with  $n$  up to  $n = 6$  ( $L = 0, 2$ ),  $n = 4$  ( $L = 1$ ) for the singlet states and  $n$  up to  $n = 4$  ( $L = 0, 2$ ) and  $n = 3$  ( $L = 1$ ) for the triplet states was performed by de Heer and coworkers [12, 16]. The assessment included all the available experimental data as well as the results of most advanced existing theoretical calculations based on the R-matrix method (29 states) [20], R-matrix-with-pseudostates method [21] and the CCC method

(69 and 75 states) [22].

In order to check (and confirm) the accuracy of these recommended data we have performed new CCC calculations for some of these transitions by employing 89 states in the expansion basis. The calculations were carried out in a pure  $LS$ -basis which is known to be very accurate for all but the  $4^{1,3} F$  terms where relativistic corrections bring about a noticeable singlet-triplet mixing<sup>1</sup>. It was found that in the majority of cases the CCC-89 results agree well with the recommended data of Ref. [12]. Some discrepancy was detected for high-energy behavior of the spin-forbidden transitions from the ground state into some  $n \geq 3$  terms. Note also that the most recent cross section measurements for the transitions  $1^1 S \rightarrow 2^{1,3} L$  [23] are in a good agreement with the CCC-89 results.

The transitions from  $n = 2$  to higher  $n$ -states, as well as the transitions between the states with  $n > 2$  were not covered in Refs.[12] and [16]. Semiempirical cross section formulae for these transitions, based on the earlier Born and semiclassical calculations, are given in Ref. [7]. There also exist systematic cross section data for transitions up to  $n = 4$  calculated within the Coulomb-Born approximation [9]. More recently, accurate cross section calculations were performed for some transitions from the ground and metastable states using the R-matrix-with-pseudostates (RMPS) method [21].

The atomic data used in the presented database can be considered as the most accurate available data on excitation of He I. The general estimate of the accuracy is close to that of Ref. [16] where cross sections of excitation from the ground state were ascribed a 10-30% accuracy for the  $\Delta S = 0$  transitions and  $\geq 30\%$  for the  $\Delta S \neq 0$  transitions. As for the transitions between the excited states, the present state of art in cross section measurements does not allow one to carry out reliable experimental determination of this parameter. The measurements of the Maxwellian rate coefficients, however, are indeed feasible [24], and we found that they agree well with

---

<sup>1</sup>Although in many experimental conditions the populations of the  $4^1 F$  and  $4^3 F$  terms quickly equilibrate, in some cases this mixing may have to be taken into account as in, e.g., Ref. [5].

the CCC-89 data. A conservative estimate for the accuracy of such cross sections is likely to be 50%.

The procedure of cross section averaging over the threshold resonances has been applied to the cross sections for all transitions. The analytic fits shown below represent the cross section with the averaged resonance structure. For a vast majority of applications, such a representation is quite sufficient; however, if very low electron temperatures ( $T_e \ll \Delta E$ ) are involved, one has to make use of the original data in order to obtain a better accuracy for the rate coefficients.

When representing the excitation cross section data in analytic form, it is customary (and more convenient) to use the collision strength  $\Omega(E/\Delta E)$  where  $E$  is the collision energy and  $\Delta E$  is the transition (threshold) energy. The relation of  $\Omega(E/\Delta E)$  to the excitation cross section  $\sigma(E, \Delta E)$  is:

$$\sigma(E, \Delta E) = \pi a_0^2 \frac{Ry}{g_i E} \Omega\left(\frac{E}{\Delta E}\right) \quad (1)$$

where  $\pi a_0^2 \approx 0.8797 \times 10^{-16} \text{ cm}^2$ ,  $g_i$  is the statistical weight of the initial state, and  $Ry \approx 13.6057 \text{ eV}$  is the Rydberg energy. The collision strength  $\Omega(x)$ ,  $x = E/\Delta E$ , for all transitions for which recommended data were generated, have been fitted to analytic expressions with a finite number of fitting parameters. The forms of these expressions for different types of transitions are given below. It should be noted also that the use of collision strengths rather than cross sections allows one to avoid some ambiguity arising in certain cases due to the non-coinciding energy thresholds in different calculations.

The collision strengths for transitions  $n_i 2S_{i+1} L_i \rightarrow n_f 2S_{f+1} L_f$  are divided into three groups, vis.:

dipole-allowed transitions ( $\Delta S = 0, \Delta L = \pm 1$ ):

$$\begin{aligned} \Omega(x) &= \left( A_1 \ln(x) + A_2 + \frac{A_3}{x} + \frac{A_4}{x^2} + \frac{A_5}{x^3} \right) \\ &\times \left( \frac{x+1}{x+A_6} \right) \end{aligned} \quad (2)$$

dipole-forbidden transitions ( $\Delta S = 0, \Delta L \neq \pm 1$ ):

$$\begin{aligned} \Omega(x) &= \left( A_1 + \frac{A_2}{x} + \frac{A_3}{x^2} + \frac{A_4}{x^3} \right) \\ &\times \left( \frac{x^2}{x^2 + A_5} \right) \end{aligned} \quad (3)$$

spin-forbidden transitions ( $\Delta S \neq 0$ ):

$$\begin{aligned} \Omega(x) &= \left( A_1 + \frac{A_2}{x} + \frac{A_3}{x^2} + \frac{A_4}{x^3} \right) \\ &\times \left( \frac{1}{x^2 + A_5} \right). \end{aligned} \quad (4)$$

The values of the fitting coefficients  $A_i$  for the  $i-f$  transitions ( $n_i, n_f \leq 4$ ) within each of three groups are given in Tables I-III for Eq. (2), (3) and (4), respectively. The accuracy of the excitation cross section within the group of states with  $n, n' \leq 4$  is generally high, although it somewhat varies with the energy. For instance, the original R-matrix results of Ref. [20] can be applied only for the electron impact energies below the ionization threshold of 24.6 eV.

In order to illustrate the quality of the used analytic fits for the recommended cross sections and the dispersion of the various original sets of data, we show in Fig. 1 the cross sections for the transition  $1^1S \rightarrow 3^1P$  taken from the NIFS database [25] and considered in the process of the data assessment. The dispersion of the data in the region of the maximum is rather large. CCC-89, RMPS [21], and RM-29 below the ionization threshold [20] are considered as giving the best theoretical results and agree very well with the most accurate experimental data (see assessment in Ref. [16]). The full line in Fig. 1 represents the fit of these theoretical data. Figures 2 and 3 provide examples for the quality of the fits and data assessment procedure for the dipole- and spin-forbidden transitions, respectively.

Although the rms deviation was calculated for each of the transitions involved, we do not present the corresponding values in the Tables I-III where the fitting coefficients for all excitation collision strengths are given. We found that large values of rms are normally due to the presence of resonances rather

than low quality of the fit, and thus they are misleading. Outside the resonance region, the accuracy of the data presented by the fit is within 5–10%.

The set of the recommended cross sections for all the transitions with  $n_i, n_f \leq 4$  are shown in the Graphs I 1-36. For a better visibility, some cross sections are shown by dashed lines.

As was mentioned in the Introduction, we use scaling relations to determine the cross sections (collision strengths) of the transitions  $n_i \rightarrow n_f$  with  $n_i \leq 3$ ,  $n_f \geq 5$  and  $n_i \geq 4$ ,  $n_f \geq 5$ . For the first group of transitions, the following scaling relation is suggested:

$$\sigma(n_i^{2S_i+1} L_i - n_f^{2S_f+1} L_f) = \left(\frac{4}{n_f}\right)^3 \sigma(n_i^{2S_i+1} L_i - 4^{2S_f+1} L_f) \quad (5)$$

which follows from the Born approximation for dipole-allowed transitions, and from classical considerations for the forbidden ones. If the difference  $\Delta n = n_f - n_i$  is not large, the scaling factor  $(4/n_f)^3$  is to be replaced by the ratio  $(f_{n_i l_i; n_f l_f} / f_{n_i l_i; 4l_f})$  for the optically allowed transitions, where  $f_{n_i l_i; n_f l_f}$  is the oscillator strength for the  $n_i l_i \rightarrow n_f l_f$  transition.

With respect to the transitions within the group of states  $n_i \geq 4$ ,  $n_f \geq 5$ , we consider the angular momentum states as degenerate. The following semiempirical expression for the  $\sigma(n_i \rightarrow n_f)$  cross section can be used [7]:

$$\sigma(n_i - n_f) = 3.52 \times 10^{-16} \left( \frac{Ry}{\Delta E_{n_i n_f}} \right)^2 f_{n_i n_f} F(x) \text{ (cm}^2\text{)} \quad (6)$$

where

$$F(x) = \frac{1}{x} [1 - \exp(-\xi(x+1)) \ln(x+0.2)], \quad (7)$$

$$x = \frac{E}{\Delta E_{n_i n_f}}, \quad \xi = \frac{1}{2} \left( f_{n_i n_f} \frac{Ry}{\Delta E_{n_i n_f}} \right)^{-0.7} \quad (8)$$

and  $\Delta E_{n_i n_f}$  and  $f_{n_i n_f}$  are the transition energy and the oscillator strength for the  $n_i - n_f$  transition, respectively. (A simple and accurate expression for  $f_{n_i n_f}$  is given in Ref. [26].)

### 3 Electron impact ionization

The electron-impact cross section for single ionization of He from its ground state is well established from the threshold to very high collision energies [27, 28]. The CCC-89 results agree with the experimental data within their uncertainty (5-10%). Ionization cross section measurements from excited states of He have been performed only for the  $2^3S$  metastable state [29, 30] covering the energy range up to 1 keV and overlapping in the region 6-18 eV. The Born-type and K-matrix cross section calculations for the ionization of  $2^{1,3}S$  metastable states have also been performed in the past [15, 31, 32].

In the present work we have performed extensive CCC (89 coupled states) calculations for single ionization of the He from all excited states with  $n \leq 4$ . These cross sections have been fitted to the analytic expression:

$$\sigma_{ion}(n^{2S+1} L) = \frac{10^{-13}}{IE} \left[ A_1 \ln \frac{E}{I} + \sum_{i=2}^6 A_i \left(1 - \frac{I}{E}\right)^{i-1} \right] \text{ (cm}^2\text{)} \quad (9)$$

where  $I$  (in eV) is the ionization energy of the state  $n^{2S+1} L$ ,  $E$  (in eV) is the collision energy and  $A_i$  are the fitting coefficients. The values of the coefficients  $A_i$  for all the states considered are given in Table IV. The ionization cross sections for this group of states are shown in the Graphs II 1-6. We note that the fit for the ionization from the ground state was based on the experimental data of Ref. [28] and the present CCC-89 calculations. Figure 4 shows the experimental and theoretical data for He( $1^1S$ ) ionization together with the fitting function.

The accuracy of the present recommended data for He ionization from its excited states is believed to be within 15%.

The states with  $n \geq 5$  can be considered as degenerate and for their ionization cross sections one can use the approximate expression [7]

$$\sigma_{ion}(n; E) = 2.32 \times 10^{-16} \left( \frac{Ry}{I_n} \right)^2 \left( \frac{x-1}{x^2} \right) \ln(1.25x) \quad (cm^2) \quad (10)$$

where  $I_n$  is the (mean) ionization energy of the  $n$ -th level and  $x = E/I_n$ . Alternatively, if one wants to distinguish the  $n^{2S+1}L$  states within the same  $n$ -level, for not very high values of  $n$  ( $n \geq 5$ ), the application of the classical scaling can be suggested:

$$\sigma_{ion}(n^{2S+1}L; E) = \varepsilon^2 \sigma_{ion}(4^{2S+1}L; E/\varepsilon) \quad (11)$$

where

$$\varepsilon = \frac{I_{4LS}}{I_{nLS}} \quad (12)$$

with  $I_{nLS}$  being the ionization energy of the  $n^{2S+1}L$  state.

The double ionization of ground state helium atom has also been measured in Ref. [28] showing a maximum cross section of  $\sim 10^{-19} \text{ cm}^2$  at the energies about 250 eV. Its cross section has been fitted with an expression of the form of Eq. 9 [18] and the corresponding values of parameters  $A_i$  are given also in Table IV. The analytic fit of this cross section (with an rms of 10.5%) is shown on Fig. 12 of Ref. [18].

## 4 Acknowledgments

We are grateful to K. Bartschat for providing us with the recent RMPS data.

## References

- [1] K. Tobita, Y. Kusama, H. Nakamura, et al. Nucl. Fusion **31**, 956 (1991).

- [2] A. I. Kislyakov, V. I. Afanassiev, A. V. Khudoleev, S. S. Kozlovski and M. P. Petrov, in: *Diagnostics for Experimental Thermonuclear Fusion Reactors*, vol. 2 (Plenum Press, New York, 1998), 353.
- [3] F. B. Markus, J. M. Adams, D. V. Bartlett, et al., Plasma Phys. Control. Fusion **34**, 1371 (1992).
- [4] A. A. Korotkov and R. K. Janev, Phys. Plasmas **3**, 1512 (1996).
- [5] M Goto and T. Fujimoto *Collisional-radiative Model for Neutral Helium in Plasma: Excitation Cross Section and Singlet-triplet Wavefunction Mixing*, Rep. NIFS-DATA-43, NIFS, Nagoya (1997).
- [6] R. Arad, K. Tsigutkin, Yu.V. Ralchenko, and Y. Maron, Phys. Plasmas **7**, 3797 (2000).
- [7] T. Fujimoto, *Semiempirical Cross-sections and Rate Coefficients for Excitation and Ionization by Electron Collisions and Photoionization of Helium*, Rep. IPP-AM-8 (Institute of Plasma Physics, Nagoya University, Nagoya, 1978).
- [8] R. K. Janev, W. D. Langer, K. Evans and D. E. Post, *Elementary Processes in Hydrogen-Helium Plasmas* (Springer-Verlag, Berlin-Heidelberg, 1987).
- [9] V. A. Abramov, L. A. Vainshtein, G. I. Krotova and A. Yu. Pigarov, *Recommended Atomic Data for Hydrogen and Helium Plasmas*, Rep. INDC(CCP)-2861/GA, Nuclear Data Section, IAEA, Vienna (1988).
- [10] F. J. de Heer, R. Hoekstra, A. E. Kingston and H. P. Summers, Nucl. Fusion Suppl. Ser., **3**, 19 (1992).
- [11] See: *Atomic and Plasma-Material Interaction Data for Fusion*, vol. 3 (1992), pp. 7-87.
- [12] F. J. de Heer, *Critically Assessed Electron-Impact Excitation Cross Sections for He( $1^1S$ )*, Rep. INDC(NDS)-385, Nuclear Data Section, IAEA, Vienna (1998).

- [13] T. Kato, Y. Itikawa and K. Sakimoto, *Compilation of Excitation Cross Sections for He Atoms by Electron Impact*, Rep. NIFS-DATA-15, NIFS, Nagoya (1991).
- [14] F. J. de Heer, I. Bray, D. V. Fursa, F. W. Bliek, H. O. Folkerts, R. Hoekstra and H. P. Summers, Nucl. Fusion Suppl. Ser., **6**, 7 (1995)
- [15] I. L. Beigman, L. A. Vainshtein, M. Brix, A. Pospieszczyk, I. Bray, D. V. Fursa and Yu. V. Ralchenko, At. Data Nucl. Data Tables **74**, 123 (2000).
- [16] F. J. de Heer, R. Hoekstra, A. E. Kingston and H. P. Summers, in Ref. [11], p. 19.
- [17] I. Bray, Phys. Rev. A **49**, 1066 (1994).
- [18] T. Kato and R. K. Janev, in Ref. [11], p. 33.
- [19] I. C. Percival and D. Richards, Adv. At. Mol. Phys. **11**, 2 (1975).
- [20] P. M. J. Sawey and K. A. Berrington, At. Data Nucl. Data Tables **55**, 81 (1993).
- [21] K. Bartschat, J. Phys. B **31**, L469 (1998); private communication.
- [22] D. V. Fursa and I. Bray, J. Phys. B **30**, 757 (1997).
- [23] D. Cubric, D. J. L. Mercer, J. M. Channing, G. C. King and F. H. Read, J. Phys. B **32**, L45 (1999).
- [24] R. Denkelmann, S. Maurmann, T. Lokajczyk, P. Drepper and H.-J. Kunze, J. Phys. B **32**, 4635 (1999).
- [25] URL <http://dbshino.nifs.ac.jp/>.
- [26] L. C. Johnson, Astroph. J. **1174**, 227 (1972).
- [27] R. G. Montague, M. F. A. Harrison and A. C. H. Smith, J. Phys. B **17**, 3295 (1984).
- [28] M. B. Shah, D. S. Elliot, P. McCallion and H. B. Gilbody, J. Phys. B **21**, 2756 (1988).
- [29] D. R. Long and R. Geballe, Phys. Rev. A **1**, 260 (1970).
- [30] A. J. Dixon, M. F. A. Harrison and A. C. G. Smith, J. Phys. B **9**, 2617 (1976).
- [31] J. S. Briggs and Y. K. Kim, Phys. Rev. A **3**, 1342 (1971).
- [32] I. R. Taylor, A. E. Kingston and K. L. Bell, J. Phys. B **12**, 3093 (1979).

## Explanation of tables

**Table I.** Fit parameters for dipole-allowed collision strengths (electron impact excitation).

$i$  Initial term  
 $f$  Final term  
 $A_1, \dots, A_6$  Fit parameters  $A_1, \dots, A_6$  in Eq. (2)

**Table II.** Fit parameters for dipole-forbidden collision strengths (electron impact excitation).

$i$  Initial term  
 $f$  Final term  
 $A_1, \dots, A_5$  Fit parameters  $A_1, \dots, A_5$  in Eq. (3)

**Table III.** Fit parameters for spin-forbidden collision strengths. (electron impact excitation).

$i$  Initial term  
 $f$  Final term  
 $A_1, \dots, A_5$  Fit parameters  $A_1, \dots, A_5$  in Eq. (4)

**Table IV.** Fit parameters for electron impact ionization cross sections.

$i$  Initial term  
 $A_1, \dots, A_6$  Fit parameters  $A_1, \dots, A_6$  in Eq. (9)

## Figure Captions

Figure 1. Dipole-allowed excitation cross section  $1^1S - 3^1P$  (data from the NIFS database [25]) and fit results (collision strength calculated from Eq. (2)).

Figure 2. Dipole-forbidden excitation cross section  $2^1S - 3^1D$  (data from the NIFS database [25]) and fit results (collision strength calculated from Eq. (3)).

Figure 3. Spin-forbidden excitation cross section  $2^3S - 4^1D$  (data from the NIFS database [25]) and fit results (collision strength calculated from Eq. (4)).

## Graphs

Graphs I 1-36. Recommended electron impact excitation cross sections for transitions between atomic terms of He I with  $n_i, n'_f \leq 4$ .

Graphs II 1-6. Recommended electron impact ionization cross sections from atomic terms of He I with  $n \leq 4$ .

## Tables

Table I. Fit coefficients for the dipole-allowed excitation collision strengths (Eq. (2)).

<i>i</i>	<i>f</i>	<i>A</i> <sub>1</sub>	<i>A</i> <sub>2</sub>	<i>A</i> <sub>3</sub>	<i>A</i> <sub>4</sub>	<i>A</i> <sub>5</sub>	<i>A</i> <sub>6</sub>
$1^1S$	$2^1P$	7.087E-01	-9.347E-02	-1.598E+00	2.986E+00	-1.293E+00	3.086E-01
$1^1S$	$3^1P$	1.730E-01	2.410E-02	-4.709E-01	7.690E-01	-3.209E-01	8.568E-01
$1^1S$	$4^1P$	6.923E-02	6.893E-03	-2.079E-01	3.508E-01	-1.497E-01	4.280E-02
$2^1S$	$2^1P$	3.404E+01	7.267E+01	1.710E+02	-7.033E+02	4.704E+02	1.194E+01
$2^1S$	$3^1P$	3.336E+00	-1.147E+00	-4.889E+00	2.023E+01	-1.336E+01	1.059E+01
$2^1S$	$4^1P$	8.826E-01	-3.618E-01	-1.231E+00	5.606E+00	-3.985E+00	5.890E+00
$2^1P$	$3^1S$	4.604E+00	-2.204E+00	-1.093E+01	3.893E+01	-2.440E+01	5.612E+00
$2^1P$	$3^1D$	6.255E+01	4.458E+01	-2.409E+02	4.069E+02	-1.955E+02	1.055E+01
$2^1P$	$4^1S$	5.545E-01	-4.400E-04	-6.360E-01	1.785E+00	-4.656E-01	3.675E+00
$2^1P$	$4^1D$	7.910E+00	9.449E+00	-4.534E+01	7.295E+01	-3.374E+01	5.963E+00
$3^1S$	$3^1P$	2.052E+02	3.598E+02	-2.758E+03	5.668E+03	-3.660E+03	1.922E+01
$3^1S$	$4^1P$	9.271E+00	-2.468E+00	-2.309E+01	9.929E+01	-7.446E+01	1.829E+01
$3^1D$	$3^1P$	2.932E+02	8.061E+02	1.229E+05	-9.222E+05	1.898E+06	1.134E+02
$3^1D$	$4^1F$	4.145E+02	3.149E+02	-2.065E+03	3.516E+03	-1.650E+03	2.407E+01
$3^1D$	$4^1P$	3.712E+00	2.713E+00	-5.615E+00	5.290E+00	-2.158E+00	0.000E+00
$3^1P$	$4^1S$	2.839E+01	-1.091E+01	-7.548E+01	2.545E+02	-1.695E+02	2.058E+01
$3^1P$	$4^1D$	1.629E+02	6.048E+01	-1.055E+03	2.398E+03	-1.390E+03	2.594E+01
$4^1S$	$4^1P$	6.787E+02	9.856E+02	-1.751E+04	-4.424E+03	2.284E+05	1.876E+01
$4^1D$	$4^1F$	8.606E+02	9.447E+03	1.573E+06	8.880E+07	-3.090E+09	2.356E+02
$4^1D$	$4^1P$	1.161E+03	3.649E+03	6.912E+05	-1.081E+07	5.967E+07	1.523E+02

<i>i</i>	<i>f</i>	<i>A</i> <sub>1</sub>	<i>A</i> <sub>2</sub>	<i>A</i> <sub>3</sub>	<i>A</i> <sub>4</sub>	<i>A</i> <sub>5</sub>	<i>A</i> <sub>6</sub>
$2^3S$	$2^3P$	7.696E+01	1.250E+02	4.938E+01	-4.778E+02	3.189E+02	8.157E+00
$2^3S$	$3^3P$	3.292E+00	-3.594E+00	3.934E+00	1.138E+01	-8.145E+00	3.360E+00
$2^3S$	$4^3P$	9.700E-01	-4.920E-01	1.629E+00	5.632E-01	4.405E-02	5.963E+00
$2^3P$	$3^3S$	1.929E+01	4.277E+00	-6.306E+01	1.483E+02	-6.056E+01	8.088E+00
$2^3P$	$3^3D$	1.414E+02	9.031E+01	-6.238E+02	1.183E+03	-6.424E+02	8.626E+00
$2^3P$	$4^3S$	2.198E+00	2.445E-01	-4.386E-01	-1.691E+00	7.824E+00	4.614E+00
$2^3P$	$4^3D$	2.209E+01	2.204E+01	-1.161E+02	2.050E+02	-1.064E+02	5.876E+00
$3^3S$	$3^3P$	4.881E+02	7.567E+02	-6.376E+03	1.258E+04	-7.062E+03	1.652E+01
$3^3S$	$4^3P$	7.079E+00	-9.037E-01	-1.830E+00	2.059E+01	-8.431E+00	2.199E+00
$3^3P$	$3^3D$	9.796E+02	1.371E+03	8.389E+04	-4.649E+05	6.375E+05	4.209E+01
$3^3P$	$4^3S$	1.233E+02	2.406E+01	-5.256E+02	1.274E+03	-6.444E+02	2.301E+01
$3^3P$	$4^3D$	3.295E+02	6.359E+01	-1.630E+03	4.159E+03	-2.512E+03	2.522E+01
$3^3D$	$4^3F$	1.255E+03	8.455E+02	-6.966E+03	1.319E+04	-6.781E+03	2.291E+01
$3^3D$	$4^3P$	2.639E+01	-8.708E+00	8.497E+01	4.800E+00	-2.920E+01	4.310E+00
$4^3S$	$4^3P$	1.734E+03	2.784E+03	-4.698E+04	1.403E+05	-1.127E+05	3.854E+01
$4^3P$	$4^3D$	3.462E+03	8.765E+03	5.011E+05	-6.347E+06	1.989E+07	6.451E+01
$4^3D$	$4^3F$	2.884E+03	2.423E+04	1.663E+07	-2.552E+08	2.912E+09	5.760E+02

Table II. Fit coefficients for the dipole-forbidden collision strengths (Eq. (3)).

<i>i</i>	<i>f</i>	<i>A</i> <sub>1</sub>	<i>A</i> <sub>2</sub>	<i>A</i> <sub>3</sub>	<i>A</i> <sub>4</sub>	<i>A</i> <sub>5</sub>
$1^1S$	$2^1S$	1.888E-01	-5.754E-01	3.439E+00	-2.088E+00	2.544E+01
$1^1S$	$3^1S$	4.033E-02	-1.872E-02	2.368E+00	-1.379E+00	1.258E+02
$1^1S$	$3^1D$	9.708E-03	2.855E-02	-8.265E-02	4.944E-02	1.992E-01
$1^1S$	$4^1S$	1.613E-02	-5.564E-02	2.943E-01	-2.024E-01	2.342E+01
$1^1S$	$4^1D$	5.420E-03	1.198E-02	-3.173E-02	1.606E-02	1.060E-01
$1^1S$	$4^1F$	4.383E-05	-1.033E-04	3.772E-03	1.631E-02	5.644E+01
$2^1P$	$3^1P$	1.689E+01	-4.916E+01	1.185E+02	-7.711E+01	1.079E+01
$2^1P$	$4^1F$	4.731E+00	2.708E+01	-3.209E+01	1.993E+01	2.372E+01
$2^1P$	$4^1P$	3.599E+00	-1.267E+01	1.916E+01	-1.007E+01	0.000E+00
$2^1S$	$3^1S$	3.762E+00	-1.140E+01	1.403E+01	-5.377E+00	1.010E+00
$2^1S$	$3^1D$	1.058E+01	3.485E+01	7.830E+01	-1.043E+02	5.370E+01
$2^1S$	$4^1S$	7.829E-01	-2.417E+00	2.876E+00	-1.108E+00	0.000E+00
$2^1S$	$4^1D$	1.872E+00	5.458E+00	-6.857E+00	5.902E+00	3.358E+01
$2^1S$	$4^1F$	5.041E-01	4.182E+00	-6.329E+00	3.139E+00	9.425E+00
$3^1D$	$4^1S$	5.089E+00	-2.327E+01	5.943E+01	-4.074E+01	6.132E-01
$3^1D$	$4^1D$	9.109E+01	-2.982E+02	6.165E+02	-3.155E+02	1.178E+01
$3^1P$	$4^1F$	1.542E+02	7.434E+02	4.114E+02	-5.986E+02	2.059E+02
$3^1P$	$4^1P$	6.444E+01	-2.365E+02	4.775E+02	-3.084E+02	1.641E+01
$3^1S$	$3^1D$	5.183E+01	-1.322E+03	7.452E+04	-9.993E+04	1.321E+03
$3^1S$	$4^1S$	1.523E+01	-8.159E+01	1.695E+02	-9.929E+01	5.103E+00
$3^1S$	$4^1D$	2.585E+01	-8.587E+01	1.017E+02	-4.008E+01	0.000E+00
$3^1S$	$4^1F$	1.939E+01	-4.539E+01	3.911E+01	-1.204E+01	0.000E+00
$4^1S$	$4^1D$	2.148E+02	1.271E+04	1.046E+07	-1.575E+07	9.878E+04
$4^1S$	$4^1F$	3.057E+01	-1.045E+03	2.904E+04	-3.037E+04	4.012E+02
$4^1F$	$4^1P$	2.068E+02	-5.424E+04	1.854E+07	-3.077E+07	6.528E+04

<i>i</i>	<i>f</i>	<i>A</i> <sub>1</sub>	<i>A</i> <sub>2</sub>	<i>A</i> <sub>3</sub>	<i>A</i> <sub>4</sub>	<i>A</i> <sub>5</sub>
$2^3S$	$3^3S$	8.344E+00	-2.658E+01	3.488E+01	-1.431E+01	0.000E+00
$2^3S$	$3^3D$	1.679E+01	5.841E+01	3.435E+02	-3.922E+02	6.290E+01
$2^3S$	$4^3S$	1.636E+00	-3.577E+00	1.959E+00	8.521E-01	0.000E+00
$2^3S$	$4^3D$	4.063E+00	1.541E+01	6.089E+01	-7.115E+01	5.762E+01
$2^3S$	$4^3F$	5.676E-01	4.383E+00	9.326E+00	-9.539E+00	1.816E+01
$2^3P$	$3^3P$	4.512E+01	-1.261E+02	2.152E+02	-6.746E+01	4.133E+00
$2^3P$	$4^3P$	9.110E+00	-2.180E+01	2.242E+01	-5.746E+00	0.000E+00
$2^3P$	$4^3F$	9.560E+00	5.997E+01	3.657E+01	-5.017E+01	3.155E+01
$3^3S$	$3^3D$	1.556E+02	-1.686E+03	4.257E+04	-4.764E+04	2.347E+02
$3^3S$	$4^3S$	3.862E+01	-1.898E+02	3.639E+02	-5.587E+01	1.719E+01
$3^3S$	$4^3D$	3.031E+01	1.193E+02	1.209E+02	-1.560E+02	5.758E+01
$3^3S$	$4^3F$	3.902E+01	1.083E+02	8.382E+02	-8.417E+02	4.843E+01
$3^3P$	$4^3F$	4.062E+02	1.633E+03	6.407E+03	-5.657E+03	1.825E+02
$3^3P$	$4^3P$	1.832E+02	-8.062E+02	1.381E+03	-7.116E+02	2.103E+00
$3^3D$	$4^3S$	2.782E+01	9.856E+01	8.697E+02	2.306E+03	1.772E+02
$3^3D$	$4^3D$	2.774E+02	-8.107E+02	3.733E+03	-2.662E+03	3.313E+01
$4^3S$	$4^3D$	5.093E+02	-1.954E+03	2.489E+03	-1.035E+03	0.000E+00
$4^3S$	$4^3F$	1.047E+02	-1.941E+03	2.306E+04	-2.258E+04	9.136E+01
$4^3P$	$4^3F$	6.768E+02	-6.926E+04	7.596E+06	-1.069E+07	8.532E+03

Table III. Fit coefficients for the spin-forbidden collision strengths.

<i>i</i>	<i>f</i>	<i>A</i> <sub>1</sub>	<i>A</i> <sub>2</sub>	<i>A</i> <sub>3</sub>	<i>A</i> <sub>4</sub>	<i>A</i> <sub>5</sub>
1 <sup>1</sup> S	2 <sup>3</sup> P	2.823E-01	2.048E+00	5.287E+00	-7.363E+00	2.728E+01
1 <sup>1</sup> S	2 <sup>3</sup> S	6.888E-01	1.975E-01	7.232E+00	-4.839E+00	5.003E+01
1 <sup>1</sup> S	3 <sup>3</sup> D	3.172E-03	2.325E-02	-5.084E-02	2.441E-02	-9.854E-01
1 <sup>1</sup> S	3 <sup>3</sup> P	6.730E-02	5.465E-01	-4.434E-01	-1.042E-01	1.140E+01
1 <sup>1</sup> S	3 <sup>3</sup> S	9.392E-02	-1.641E-01	7.605E-02	-4.536E-03	-9.246E-01
1 <sup>1</sup> S	4 <sup>3</sup> D	1.334E-03	1.819E-02	-3.848E-02	1.896E-02	-9.893E-01
1 <sup>1</sup> S	4 <sup>3</sup> F	0.000E+00	4.079E-04	-3.863E-04	1.701E-05	-9.497E-01
1 <sup>1</sup> S	4 <sup>3</sup> P	2.585E-02	2.275E-01	-5.827E-02	-1.615E-01	1.505E+01
1 <sup>1</sup> S	4 <sup>3</sup> S	3.008E-02	-3.956E-02	-1.940E-03	1.154E-02	-9.813E-01
2 <sup>1</sup> P	3 <sup>3</sup> D	1.702E+01	1.484E+03	-4.593E+02	-8.789E+02	3.229E+02
2 <sup>1</sup> P	3 <sup>3</sup> P	1.093E+01	8.331E+03	1.929E+04	-1.731E+04	5.540E+03
2 <sup>1</sup> P	3 <sup>3</sup> S	4.980E+00	4.415E+02	1.002E+03	-8.063E+02	5.626E+02
2 <sup>1</sup> P	4 <sup>3</sup> D	3.686E+00	1.887E+02	-9.472E+00	-1.471E+02	1.729E+02
2 <sup>1</sup> P	4 <sup>3</sup> F	8.678E-01	3.062E+01	-3.479E+01	1.127E+01	3.760E+01
2 <sup>1</sup> P	4 <sup>3</sup> P	2.243E+00	5.624E+02	8.402E+02	-3.634E+02	1.504E+03
2 <sup>1</sup> P	4 <sup>3</sup> S	6.494E-01	2.526E+01	-1.162E+00	5.160E+01	1.225E+02
2 <sup>1</sup> S	2 <sup>3</sup> P	5.983E+02	-5.310E+02	3.348E+02	-2.412E+02	2.239E+02
2 <sup>1</sup> S	3 <sup>3</sup> D	4.042E+00	1.358E+02	8.142E+01	-2.085E+02	1.737E+02
2 <sup>1</sup> S	3 <sup>3</sup> P	1.382E+00	8.314E+01	2.834E+02	-1.831E+02	3.176E+02
2 <sup>1</sup> S	3 <sup>3</sup> S	6.648E-01	1.940E+03	6.935E+02	1.447E+03	6.339E+03
2 <sup>1</sup> S	4 <sup>3</sup> D	9.480E-01	2.121E+01	-7.385E+00	-1.085E+01	7.917E+01
2 <sup>1</sup> S	4 <sup>3</sup> F	2.338E-01	-6.755E+01	8.613E+03	-8.035E+03	1.772E+04
2 <sup>1</sup> S	4 <sup>3</sup> P	2.701E-01	1.187E+01	7.598E+00	1.182E+00	1.051E+02
2 <sup>1</sup> S	4 <sup>3</sup> S	1.236E-01	2.041E+02	-2.538E+02	1.090E+03	3.582E+03

Table III (continued).

<i>i</i>	<i>f</i>	<i>A</i> <sub>1</sub>	<i>A</i> <sub>2</sub>	<i>A</i> <sub>3</sub>	<i>A</i> <sub>4</sub>	<i>A</i> <sub>5</sub>
$3^1D$	$4^3D$	4.743E+01	1.223E+05	2.074E+05	-2.893E+05	1.904E+04
$3^1D$	$4^3F$	6.314E+01	2.583E+04	-5.741E+03	-1.452E+04	1.536E+03
$3^1D$	$4^3P$	0.000E+00	3.369E+03	6.115E+03	-5.152E+03	8.638E+02
$3^1D$	$4^3S$	1.499E+00	1.809E+03	1.005E+03	-6.550E+02	9.339E+02
$3^1P$	$4^3D$	1.470E+01	5.349E+03	5.281E+03	-9.207E+03	1.556E+03
$3^1P$	$4^3F$	7.766E+01	1.248E+04	8.902E+03	-2.051E+04	2.003E+03
$3^1P$	$4^3P$	1.125E+01	1.295E+05	5.808E+04	-8.942E+04	4.622E+04
$3^1P$	$4^3S$	7.973E+00	5.673E+03	5.417E+03	-6.546E+03	3.901E+03
$3^1S$	$3^3D$	6.729E+02	6.022E+05	-2.032E+06	1.788E+06	2.709E+04
$3^1S$	$3^3P$	1.242E+03	1.094E+07	-2.101E+07	1.138E+07	3.429E+05
$3^1S$	$4^3D$	4.674E+00	2.273E+02	7.469E+02	-8.390E+02	2.907E+02
$3^1S$	$4^3F$	1.601E+00	1.311E+03	5.193E+02	-1.588E+03	4.897E+02
$3^1S$	$4^3P$	1.878E+00	7.168E+02	1.402E+03	6.210E+01	1.290E+03
$3^1S$	$4^3S$	1.395E+00	1.370E+04	-3.392E+04	7.064E+04	2.137E+04
$4^1D$	$4^3F$	6.489E+07	2.437E+10	-3.239E+12	9.177E+13	6.255E+06
$4^1S$	$4^3D$	9.651E+02	3.404E+07	-1.015E+08	7.969E+07	1.764E+06
$4^1S$	$4^3F$	2.102E+02	8.995E+05	-2.902E+06	2.495E+06	3.244E+04
$4^1S$	$4^3P$	2.968E+03	1.709E+08	-4.113E+08	3.782E+08	4.486E+06
$2^3P$	$2^1P$	7.477E+03	-7.356E+01	-1.484E+04	9.359E+03	1.364E+03
$2^3P$	$3^1D$	1.248E+01	8.429E+02	-7.194E+02	1.665E+02	2.114E+02
$2^3P$	$3^1P$	1.010E+01	3.349E+03	1.034E+04	-1.269E+04	3.023E+03
$2^3P$	$3^1S$	3.068E+00	1.914E+02	1.311E+03	-1.191E+03	5.774E+02
$2^3P$	$4^1D$	3.009E+00	1.194E+02	-1.716E+02	9.982E+01	9.528E+01
$2^3P$	$4^1F$	5.663E-01	1.780E+01	-3.464E+01	1.990E+01	1.573E+01
$2^3P$	$4^1P$	2.226E+00	4.009E+02	3.283E+03	-3.644E+03	1.904E+03
$2^3P$	$4^1S$	5.902E-01	1.755E+01	1.286E+01	1.786E+01	1.158E+02
$2^3S$	$2^1P$	4.893E+01	4.251E+03	-4.330E+03	1.934E+02	8.928E+02
$2^3S$	$2^1S$	5.475E+01	3.483E+05	2.345E+05	-5.090E+05	5.424E+04
$2^3S$	$3^1D$	1.854E+00	3.979E+01	4.699E+00	-2.647E+01	8.091E+01
$2^3S$	$3^1P$	1.383E+00	5.353E+01	3.937E+02	-4.378E+02	4.331E+02
$2^3S$	$3^1S$	6.561E-01	5.721E+02	2.975E+03	-1.773E+03	5.210E+03
$2^3S$	$4^1D$	5.492E-01	8.462E+00	-1.079E+01	5.007E+00	3.464E+01
$2^3S$	$4^1F$	8.208E-02	-1.311E+01	1.155E+03	-1.001E+03	5.398E+03
$2^3S$	$4^1P$	3.412E-01	9.770E+00	2.173E+02	-2.240E+02	5.031E+02
$2^3S$	$4^1S$	1.694E-01	7.331E+01	8.903E+01	1.828E+02	2.183E+03

Table III (continued).

<i>i</i>	<i>f</i>	<i>A</i> <sub>1</sub>	<i>A</i> <sub>2</sub>	<i>A</i> <sub>3</sub>	<i>A</i> <sub>4</sub>	<i>A</i> <sub>5</sub>
$3^3D$	$3^1D$	1.136E+09	2.017E+12	-1.201E+15	1.669E+17	1.343E+08
$3^3D$	$3^1P$	8.097E+04	-7.012E+05	2.225E+06	-2.064E+06	8.385E+03
$3^3D$	$4^1D$	4.723E+01	1.223E+05	2.166E+05	-2.717E+05	1.935E+04
$3^3D$	$4^1F$	6.305E+01	2.582E+04	-1.481E+04	-5.014E+03	1.496E+03
$3^3D$	$4^1P$	0.000E+00	2.958E+03	6.343E+03	-9.301E+03	9.406E+02
$3^3D$	$4^1S$	6.079E-01	9.783E+02	1.616E+03	-1.574E+03	8.714E+02
$3^3P$	$3^1D$	6.039E+03	4.209E+07	-1.969E+08	2.637E+08	2.223E+05
$3^3P$	$3^1P$	6.013E+03	-1.055E+04	1.091E+04	-6.078E+03	8.163E+02
$3^3P$	$4^1D$	7.376E+00	2.988E+03	8.028E+03	-7.799E+03	1.065E+03
$3^3P$	$4^1F$	6.272E+01	6.842E+03	1.574E+03	-5.607E+03	1.122E+03
$3^3P$	$4^1P$	2.776E+01	-8.087E+01	3.210E+02	-2.668E+02	2.334E+01
$3^3P$	$4^1S$	3.483E+00	1.338E+03	5.297E+03	-2.062E+03	2.147E+03
$3^3S$	$3^1D$	1.545E+02	4.931E+04	4.578E+04	-9.484E+04	6.629E+03
$3^3S$	$3^1P$	8.167E+01	8.655E+04	-5.278E+04	-4.450E+04	1.313E+04
$3^3S$	$3^1S$	1.731E+02	2.350E+06	5.044E+06	-7.406E+06	3.601E+05
$3^3S$	$4^1D$	3.036E+00	-2.081E+03	6.538E+05	-5.498E+05	1.362E+05
$3^3S$	$4^1F$	9.155E-01	6.187E+02	2.079E+02	-6.677E+02	3.049E+02
$3^3S$	$4^1P$	1.725E+00	4.197E+02	1.477E+03	-1.845E+03	1.186E+03
$3^3S$	$4^1S$	9.802E-01	7.696E+03	-2.354E+04	4.408E+04	1.801E+04
$4^3D$	$4^1D$	1.055E+09	-3.116E+11	7.151E+13	-5.541E+15	7.344E+07
$4^3D$	$4^1F$	1.828E+07	4.946E+12	-6.367E+14	1.475E+16	5.281E+08
$4^3D$	$4^1P$	3.467E+05	-1.223E+05	-1.174E+07	2.974E+07	7.585E+04
$4^3F$	$4^1F$	1.026E+10	3.470E+13	-2.933E+16	5.666E+18	6.300E+08
$4^3F$	$4^1P$	2.520E+05	-1.057E+06	-1.446E+06	8.086E+06	4.052E+04
$4^3P$	$4^1D$	1.466E+04	8.679E+08	-3.528E+09	4.055E+09	4.533E+06
$4^3P$	$4^1F$	1.878E+04	4.402E+07	-2.107E+08	2.660E+08	2.108E+05
$4^3P$	$4^1P$	1.482E+04	-4.752E+04	3.964E+04	3.244E+03	2.200E+03
$4^3S$	$4^1D$	2.220E+02	3.024E+06	9.322E+06	-1.334E+07	4.572E+05
$4^3S$	$4^1F$	4.678E+01	7.677E+04	-1.273E+05	6.421E+04	5.849E+03
$4^3S$	$4^1P$	1.650E+02	1.455E+06	-2.740E+06	1.284E+06	1.720E+05
$4^3S$	$4^1S$	3.429E+02	9.919E+06	-7.244E+06	3.127E+07	1.147E+06

Table IV. Fit coefficients for electron impact single and double ionization cross sections.

<i>i</i>	<i>A</i> <sub>1</sub>	<i>A</i> <sub>2</sub>	<i>A</i> <sub>3</sub>	<i>A</i> <sub>4</sub>	<i>A</i> <sub>5</sub>	<i>A</i> <sub>6</sub>
$1^1S$	5.857E-01	-4.457E-01	7.680E-01	-2.521E+00	3.317E+00	0.000E+00
$2^3S$	2.427E-01	-1.900E-01	3.205E-01	7.631E-01	-8.329E-01	-2.405E-01
$2^1S$	3.076E-01	-2.748E-01	4.462E-01	-1.841E-01	1.336E+00	-1.775E+00
$2^3P$	2.104E-01	-1.750E-01	2.994E-01	9.493E-01	-4.479E-01	-3.833E-01
$2^1P$	2.068E-01	-2.034E-01	5.759E-01	-2.442E-01	1.986E+00	-2.019E+00
$3^3S$	1.878E-01	-1.871E-01	1.223E+00	-3.805E+00	8.412E+00	-5.872E+00
$3^1S$	1.787E-01	-1.775E-01	7.023E-01	-1.132E+00	3.727E+00	-3.255E+00
$3^3P$	2.694E-01	-2.606E-01	6.476E-01	-2.256E+00	5.876E+00	-4.273E+00
$3^3D$	8.034E-02	-7.667E-02	8.839E-01	-4.051E+00	1.110E+01	-7.427E+00
$3^1D$	9.637E-02	-9.370E-02	1.051E+00	-4.831E+00	1.251E+01	-8.287E+00
$3^1P$	1.654E-01	-1.640E-01	3.123E-01	-4.326E-02	1.729E+00	-1.691E+00
$4^3S$	9.429E-02	-7.480E-02	8.668E-01	-3.637E+00	8.681E+00	-5.816E+00
$4^1S$	1.206E-01	-1.136E-01	7.407E-01	-3.115E+00	7.325E+00	-4.900E+00
$4^3P$	2.128E-01	-1.957E-01	4.731E-01	-1.800E+00	3.918E+00	-2.596E+00
$4^3D$	2.507E-02	-4.722E-03	1.340E-01	7.719E-01	-4.388E-01	1.245E-01
$4^1D$	1.814E-02	1.047E-02	6.380E-02	1.172E+00	-9.804E-01	3.382E-01
$4^3F$	6.742E-03	4.431E-02	-8.945E-02	1.335E+00	4.955E-01	-1.073E+00
$4^1F$	4.340E-02	1.216E-02	3.506E-01	-1.911E+00	6.694E+00	-4.631E+00
$4^1P$	1.807E-01	-1.724E-01	2.448E-01	-6.578E-01	2.026E+00	-1.535E+00
double	1.323E-06	8.208E-03	-6.676E-02	2.978E-01	-1.925E-01	0.000E+00

Electron impact excitation  $1^1S - 3^1P$

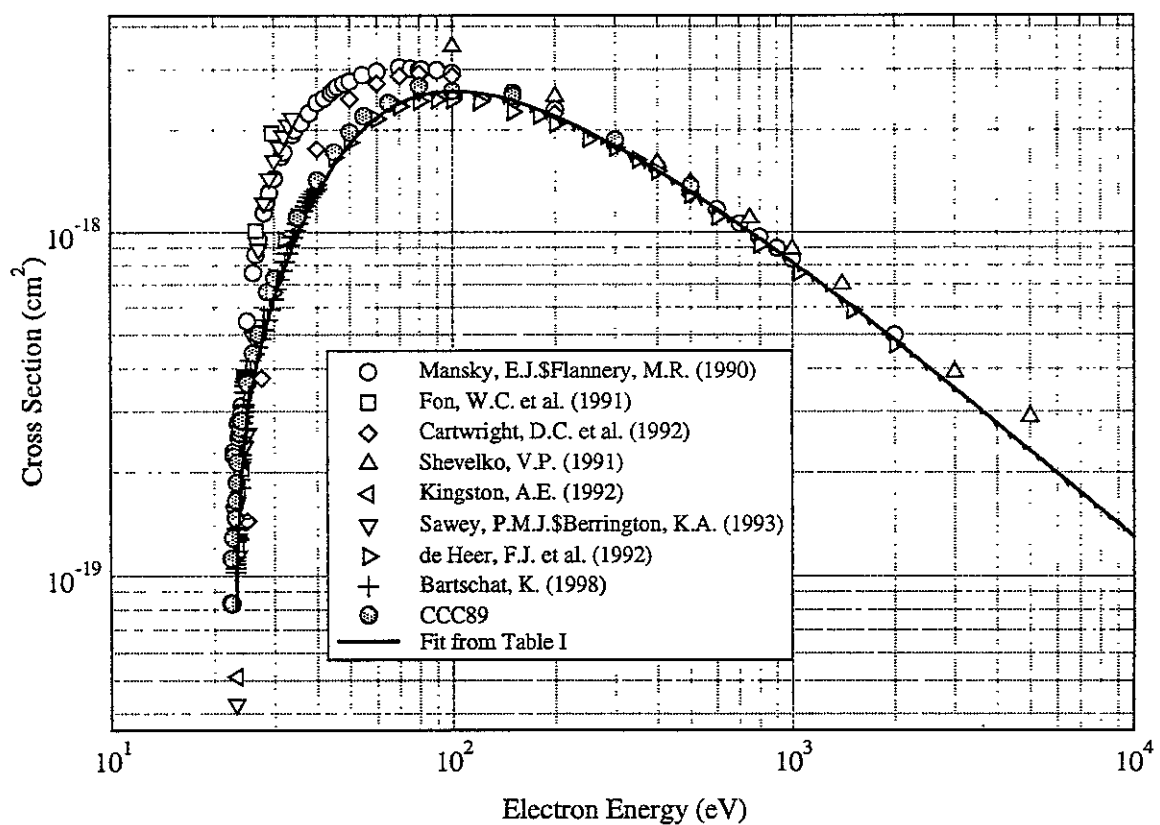


Fig. 1

Electron impact excitation  $2^1S - 3^1D$

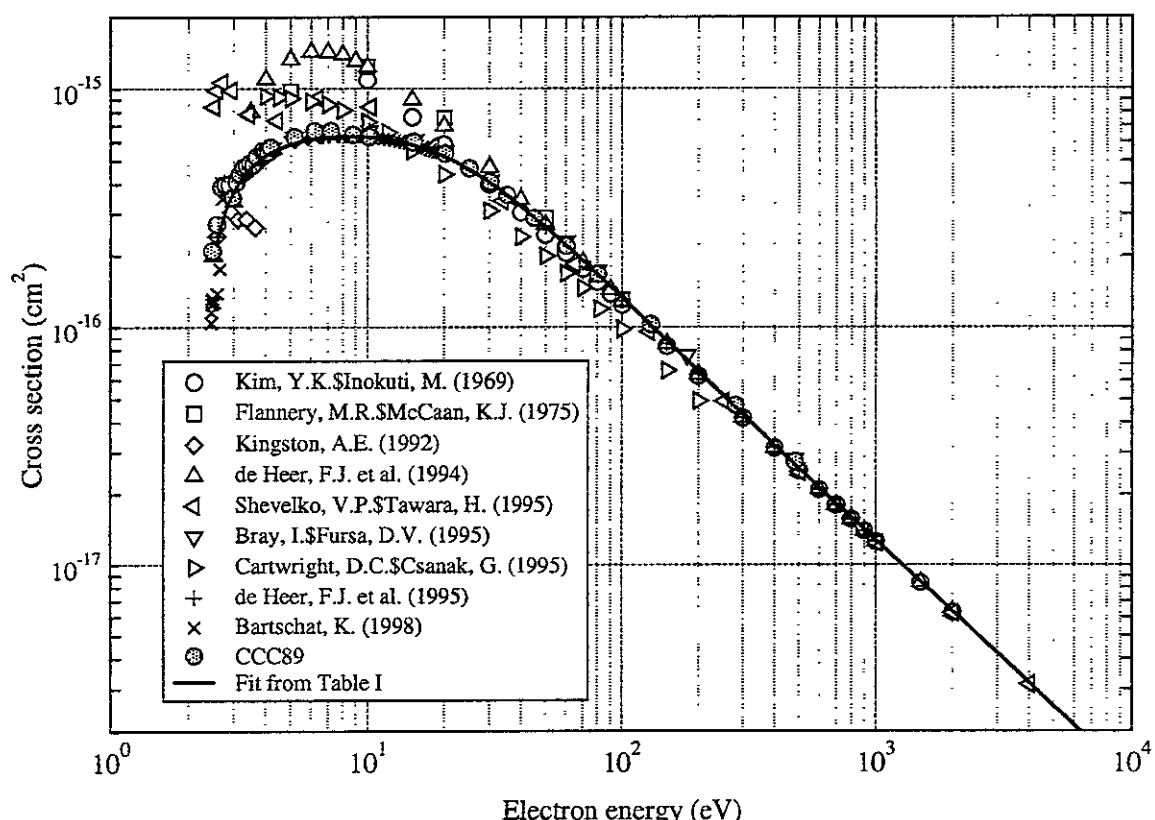


Fig. 2

### Electron impact excitation $2^3S - 4^1D$

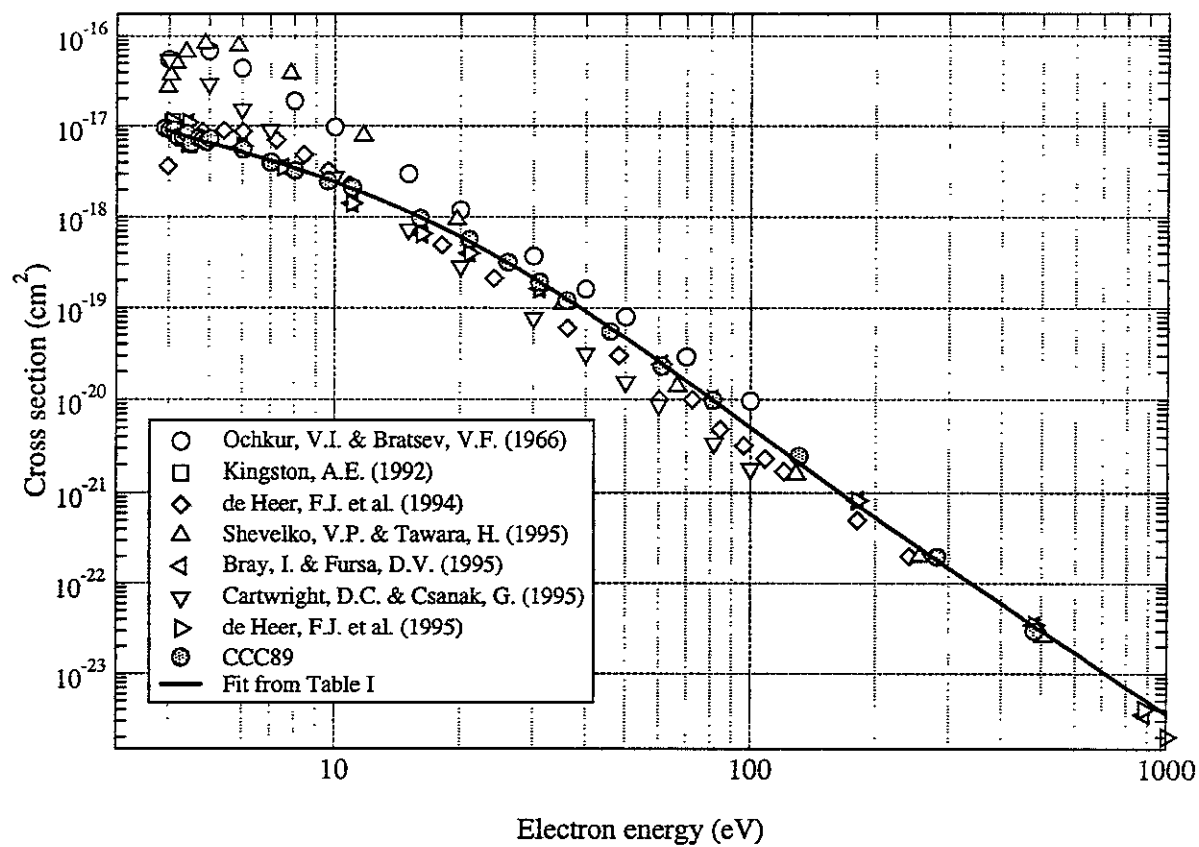


Fig. 3

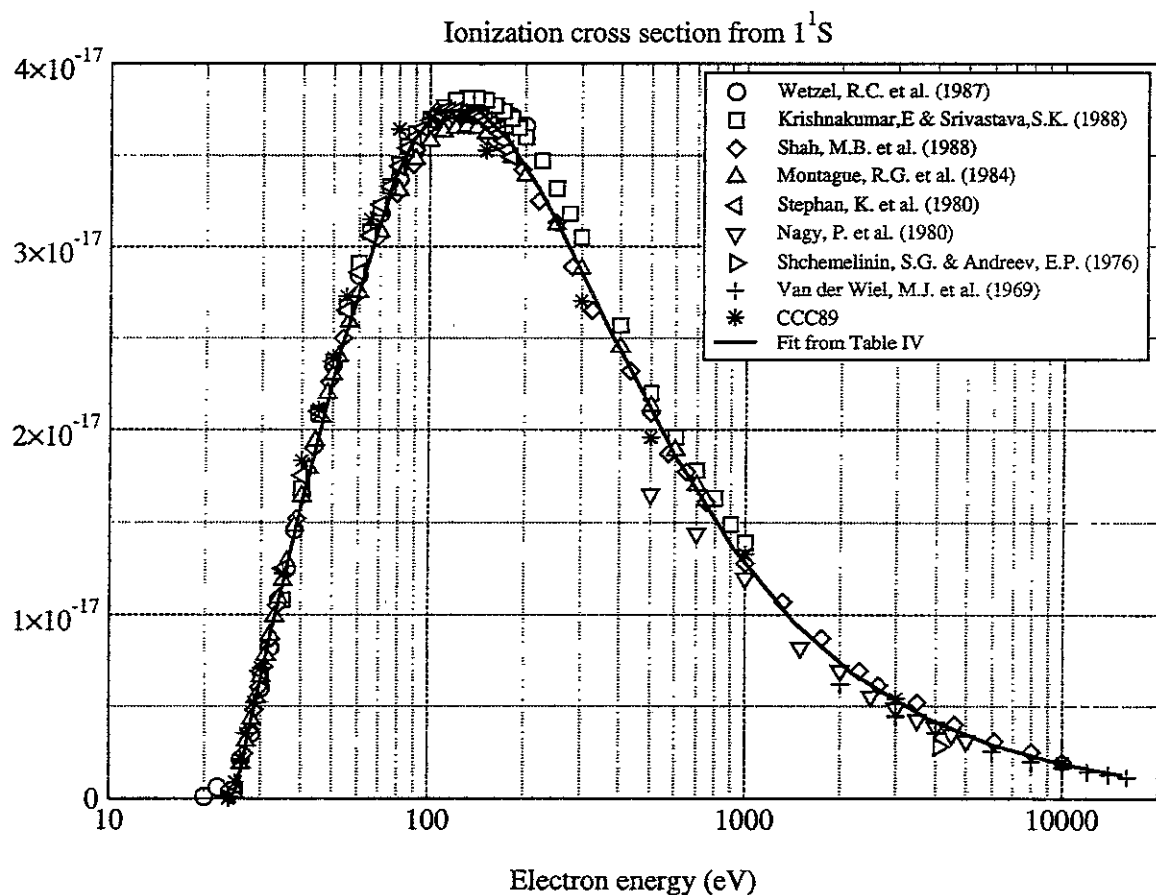
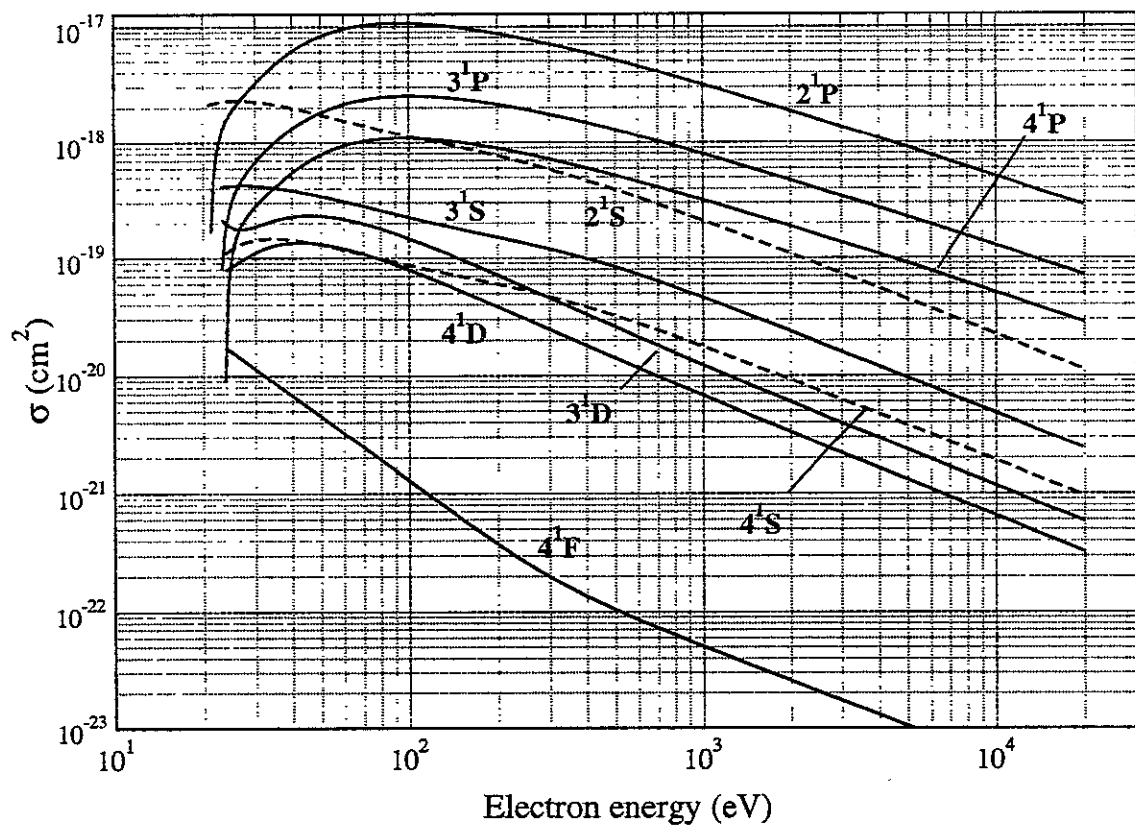


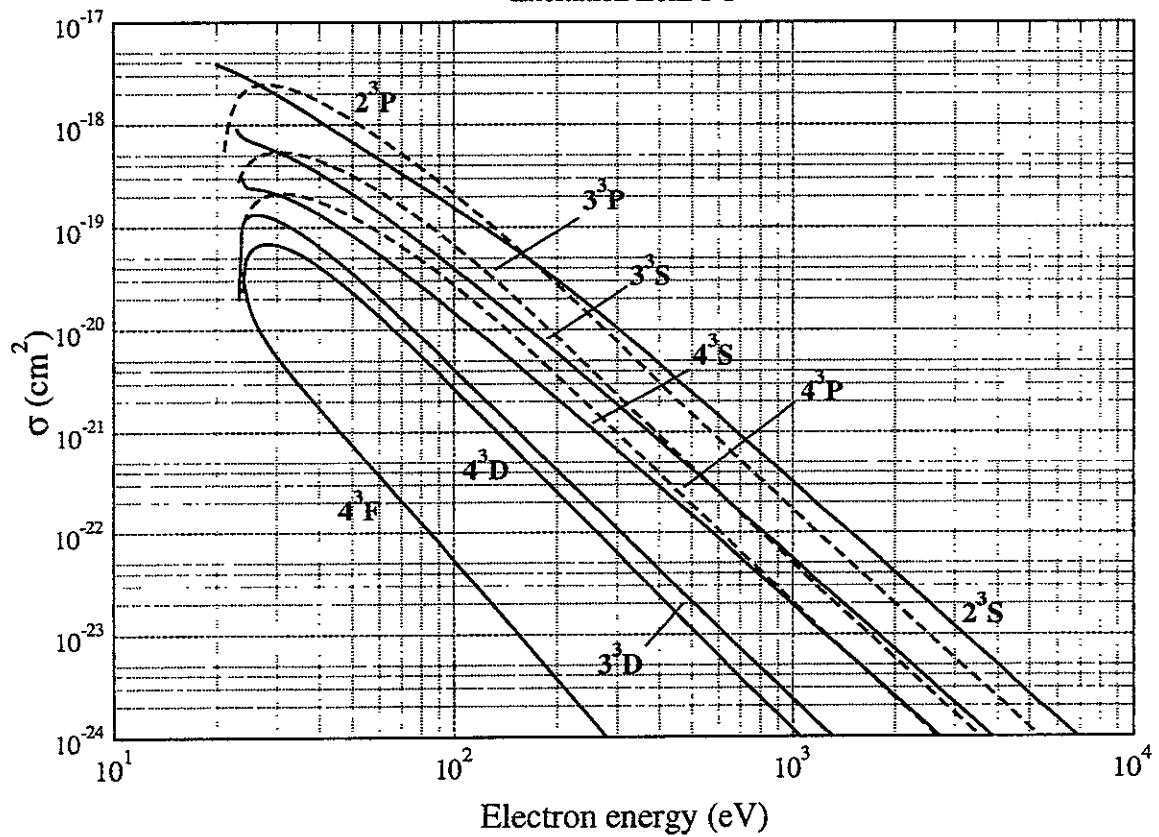
Fig. 4

Excitation from  $1^1S$

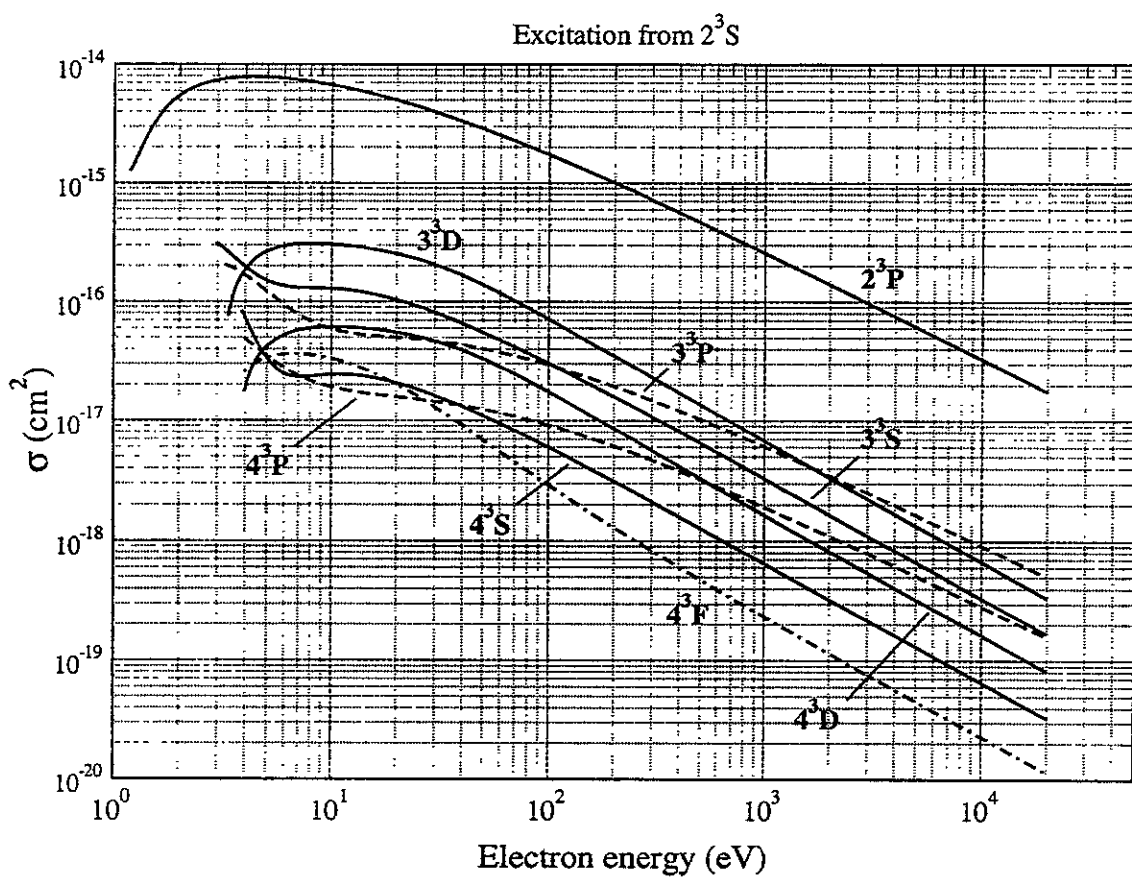


Graphs I 1

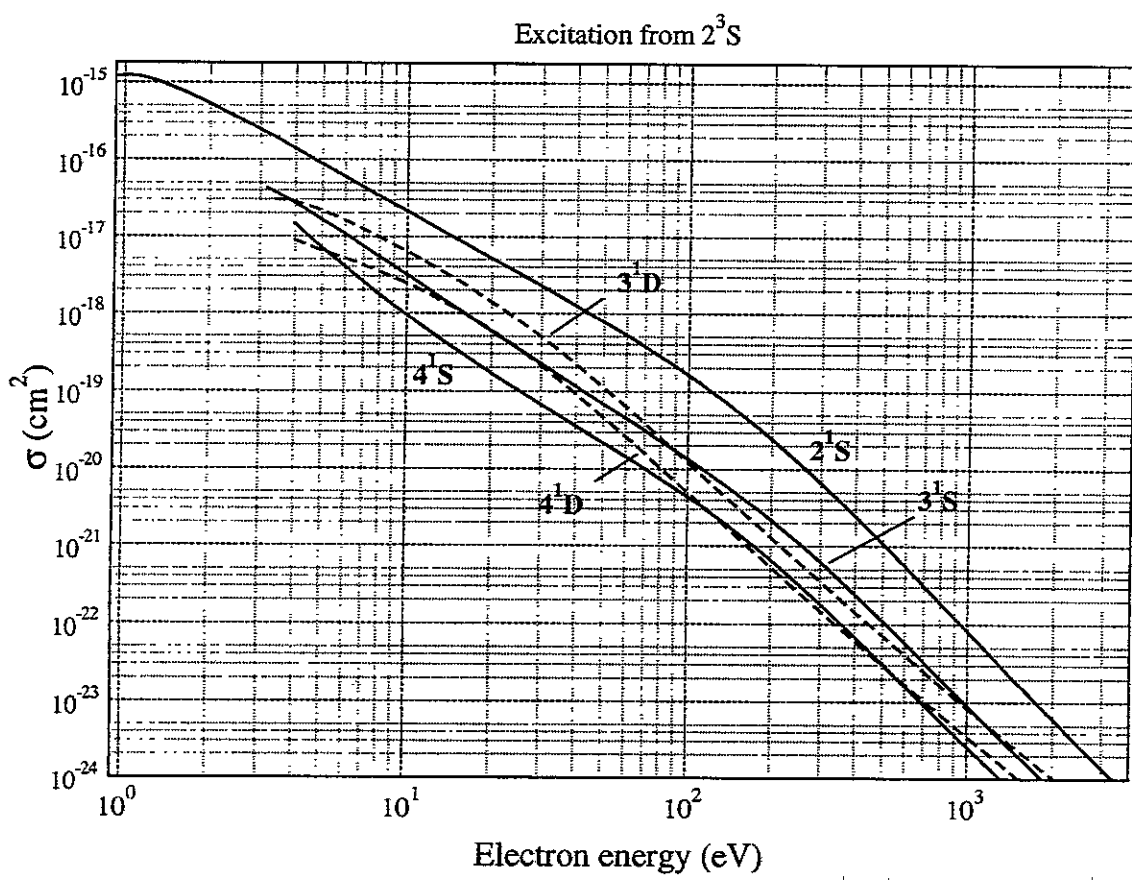
Excitation from  $1^1S$



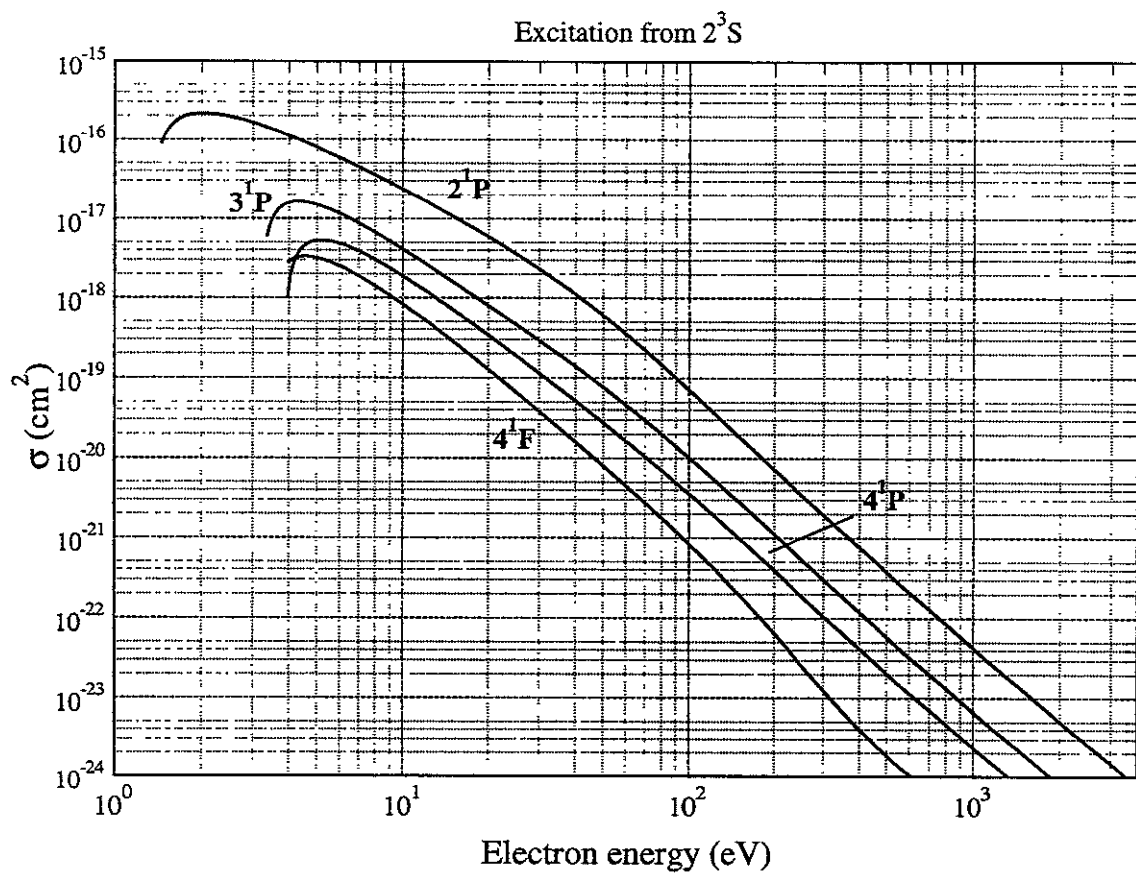
Graphs I 2



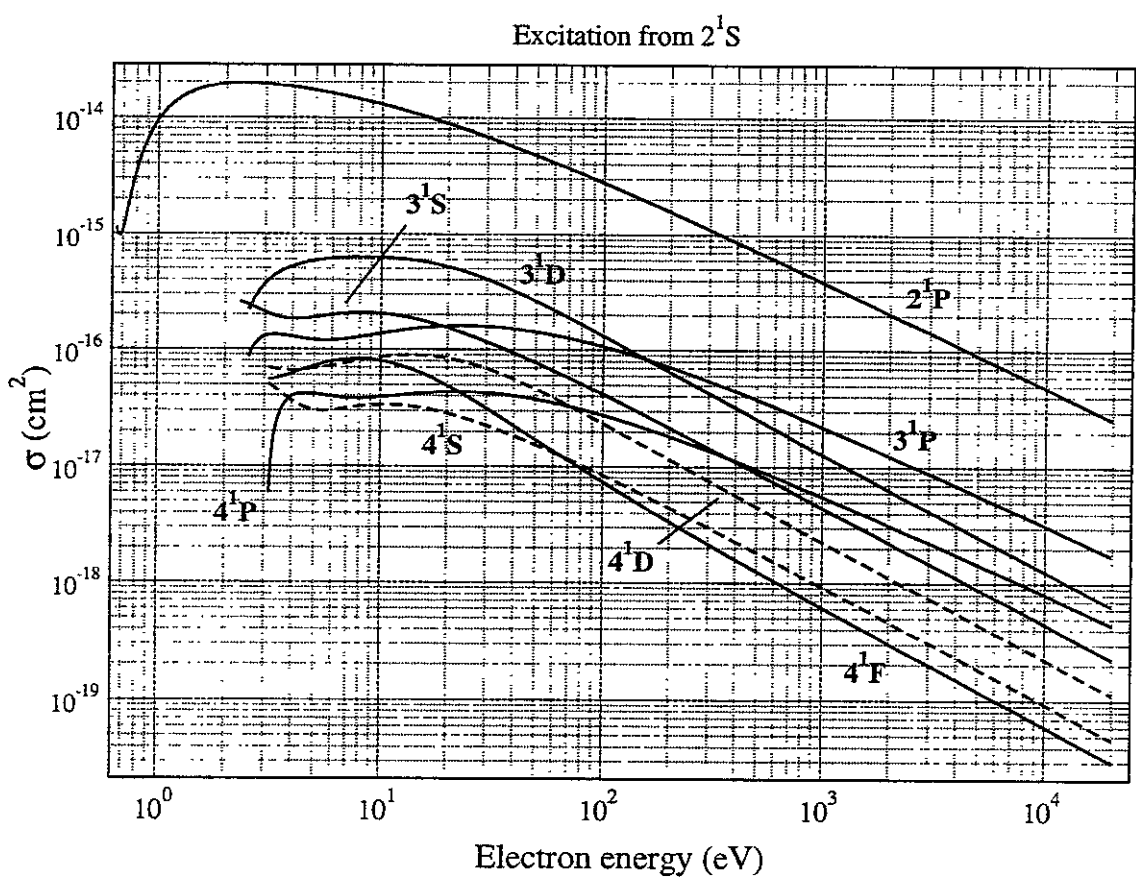
Graphs I 3



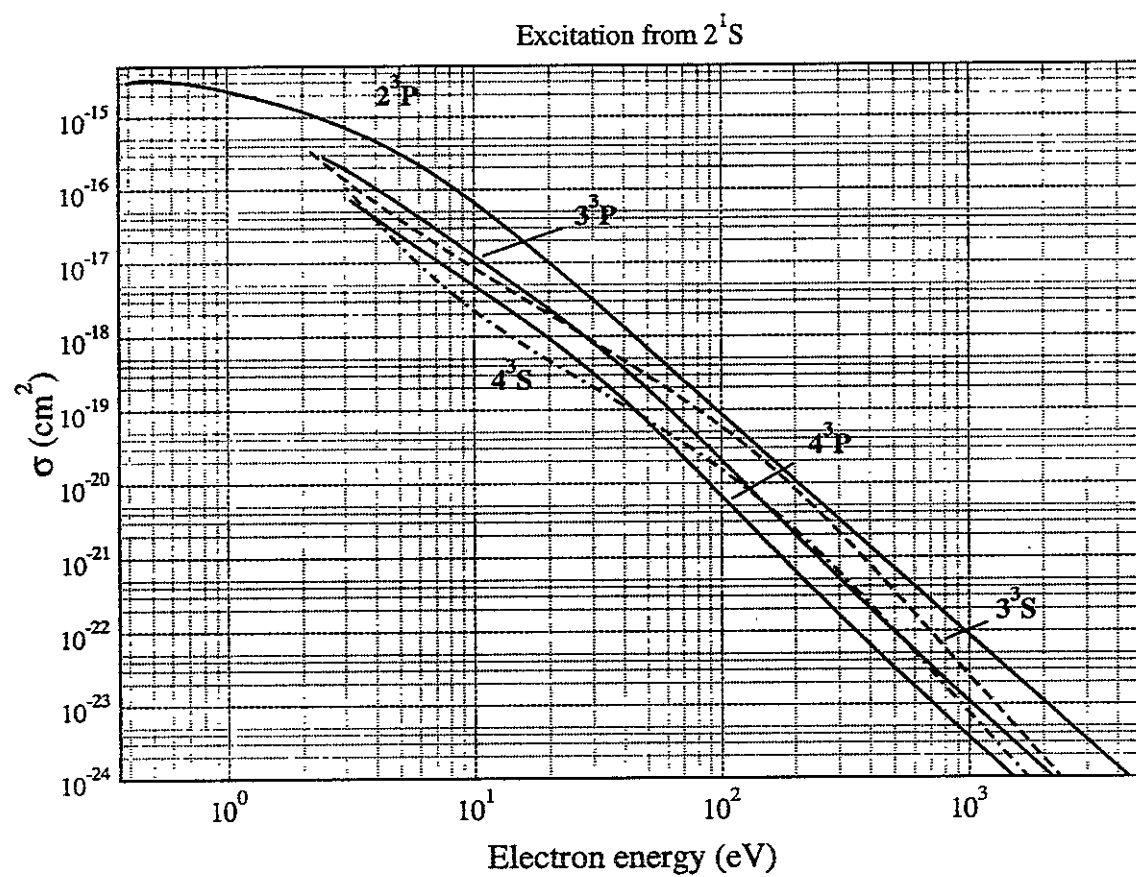
Graphs I 4



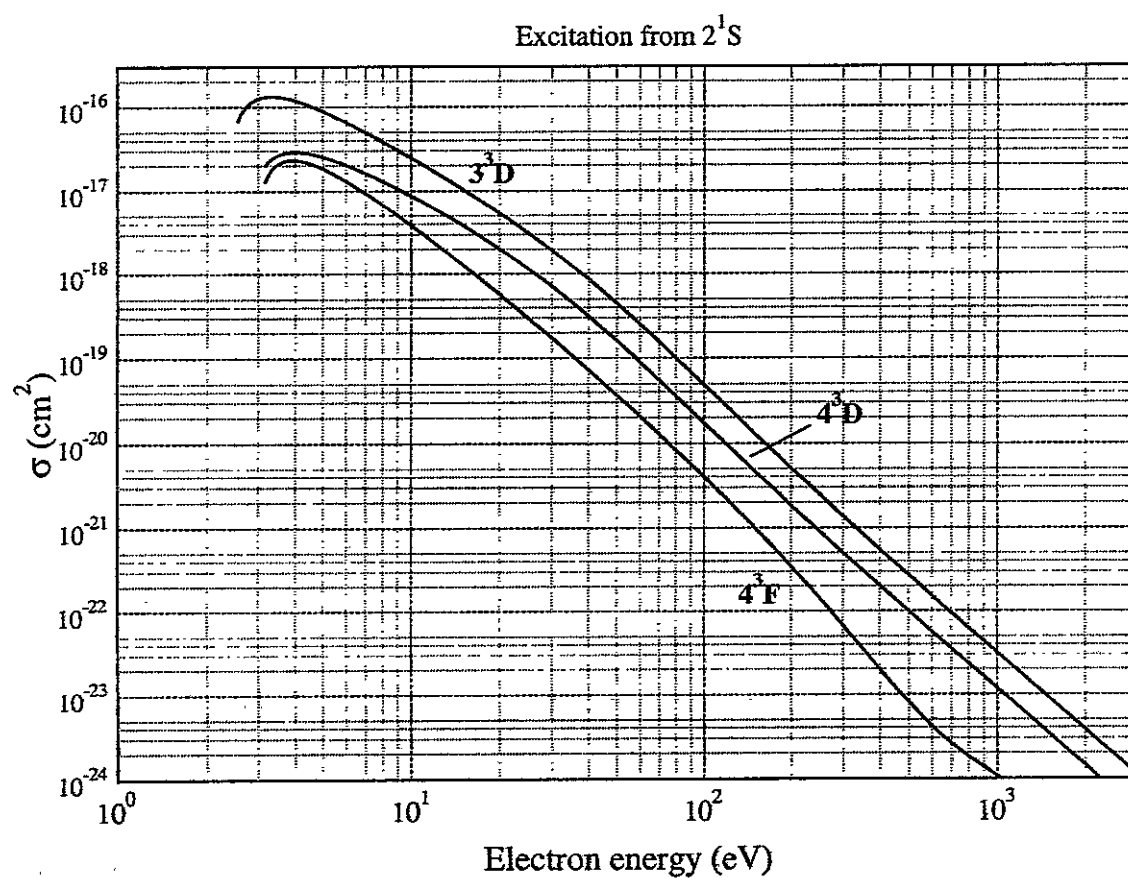
Graphs I 5



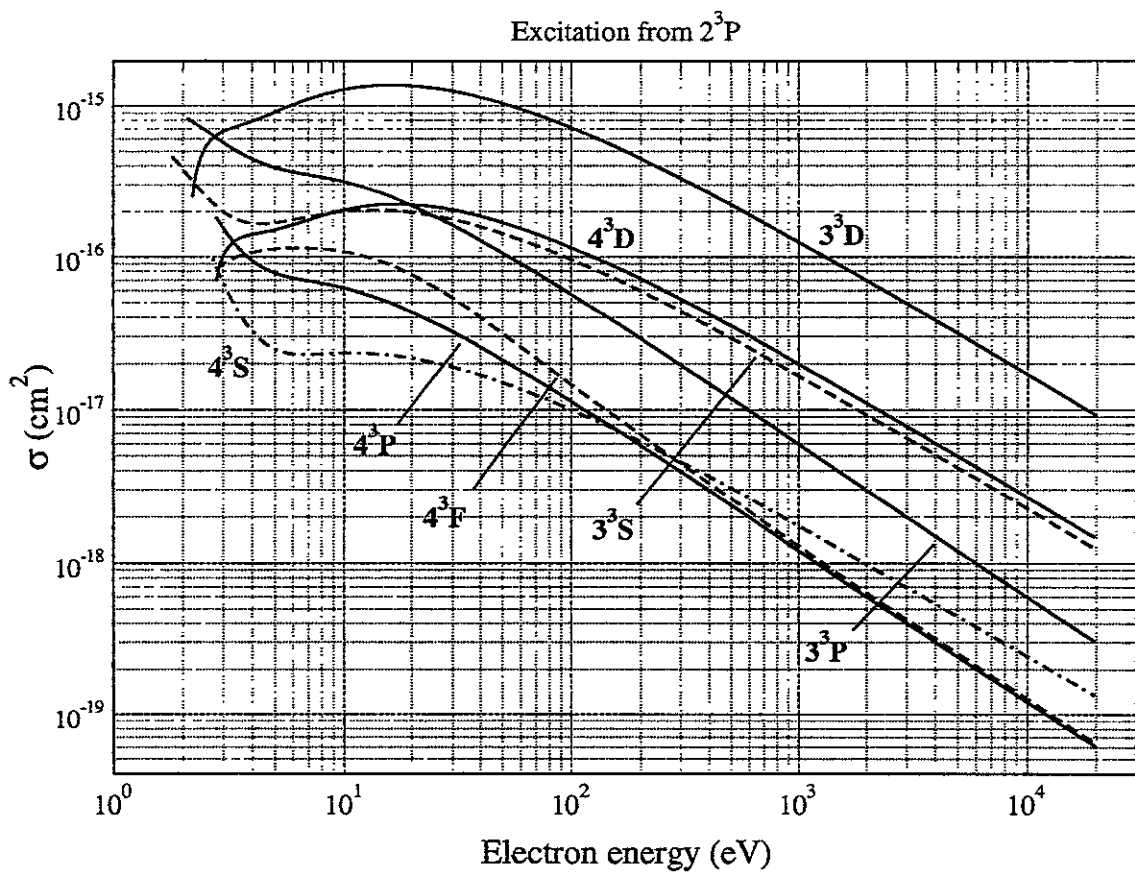
Graphs I 6



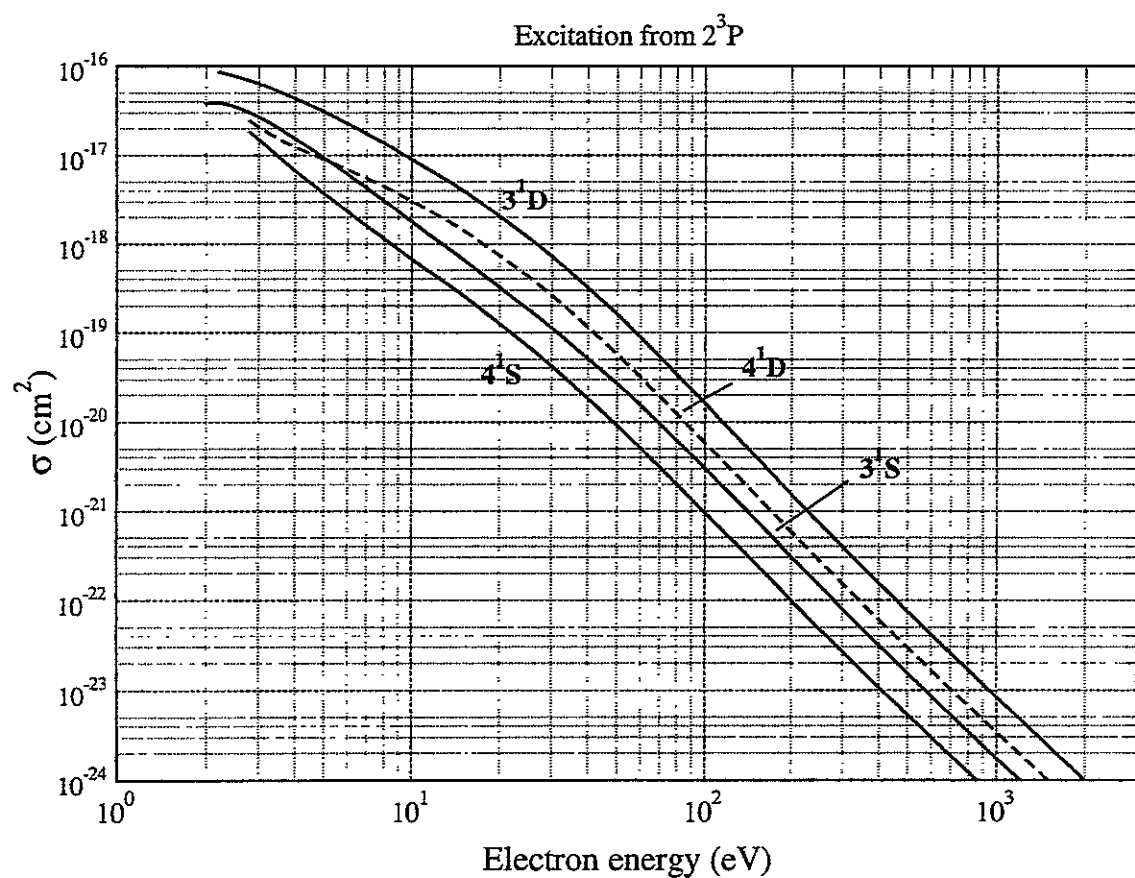
Graphs I 7



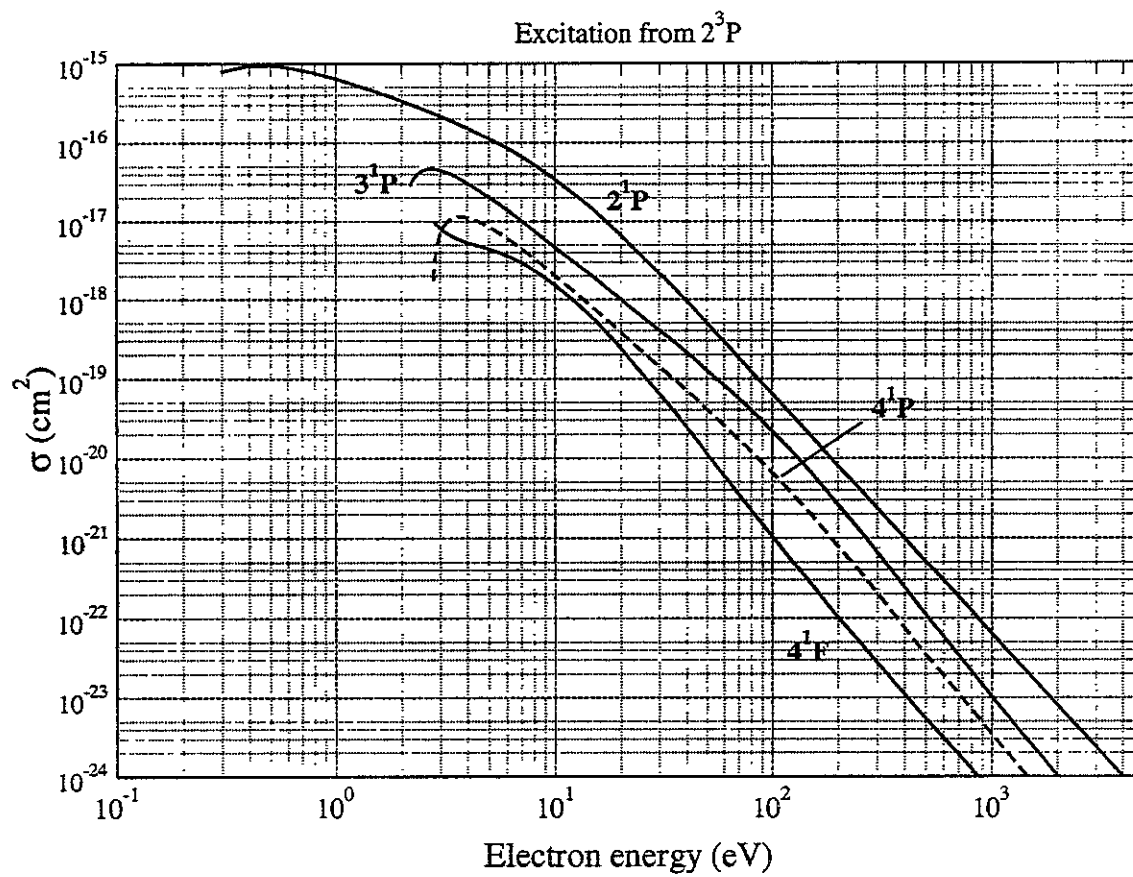
Graphs I 8



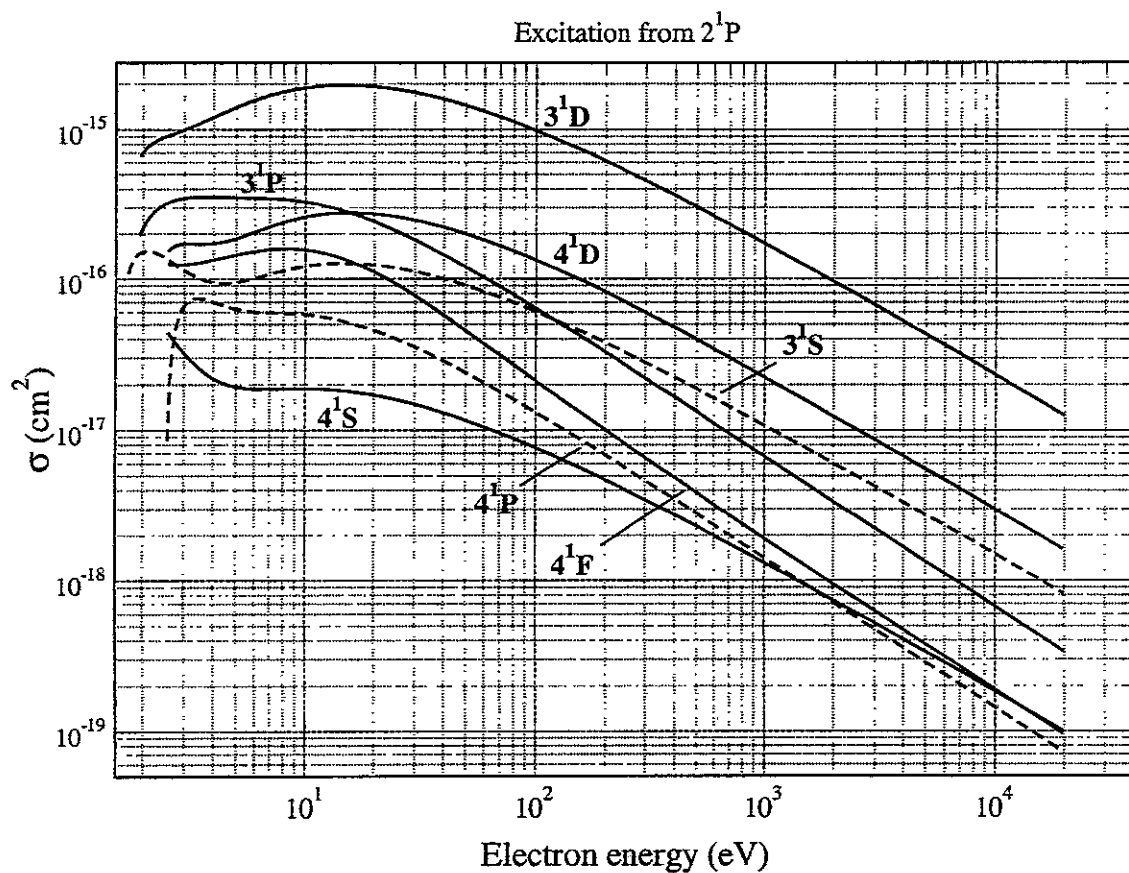
Graphs I 9



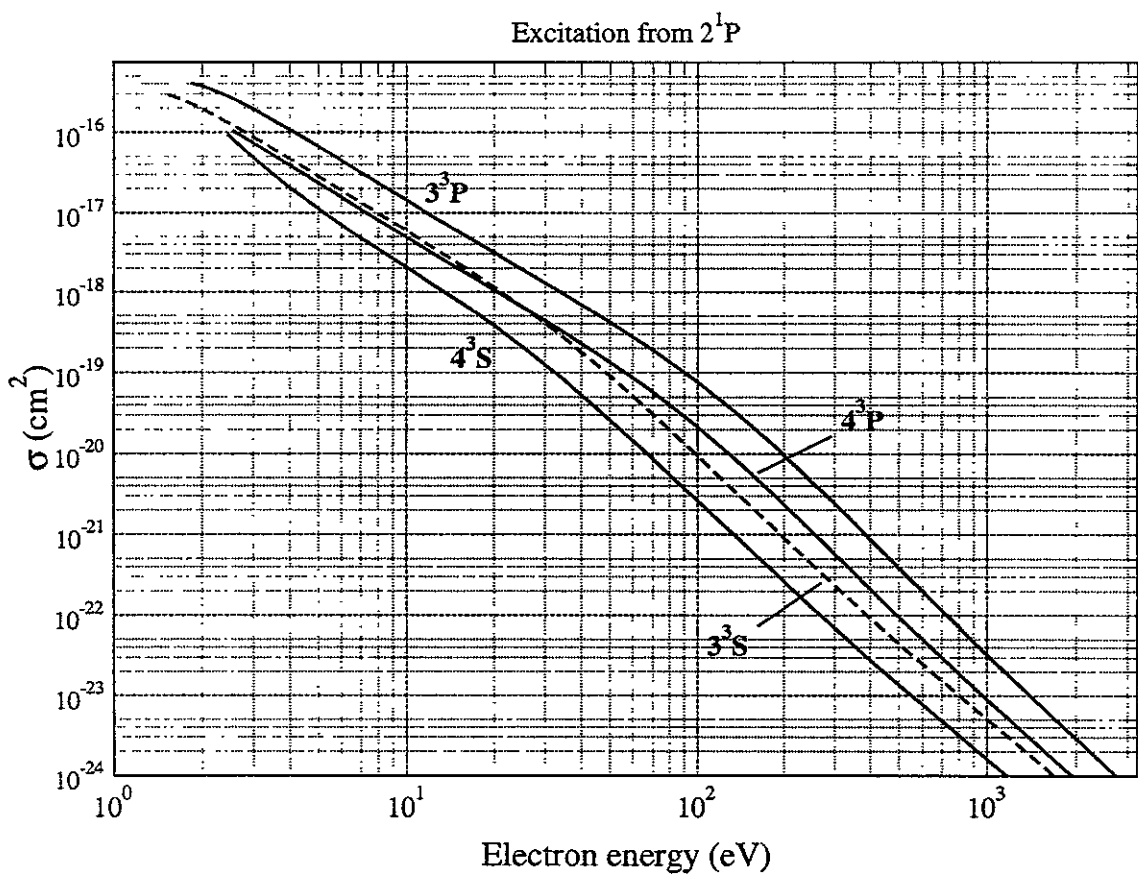
Graphs I 10



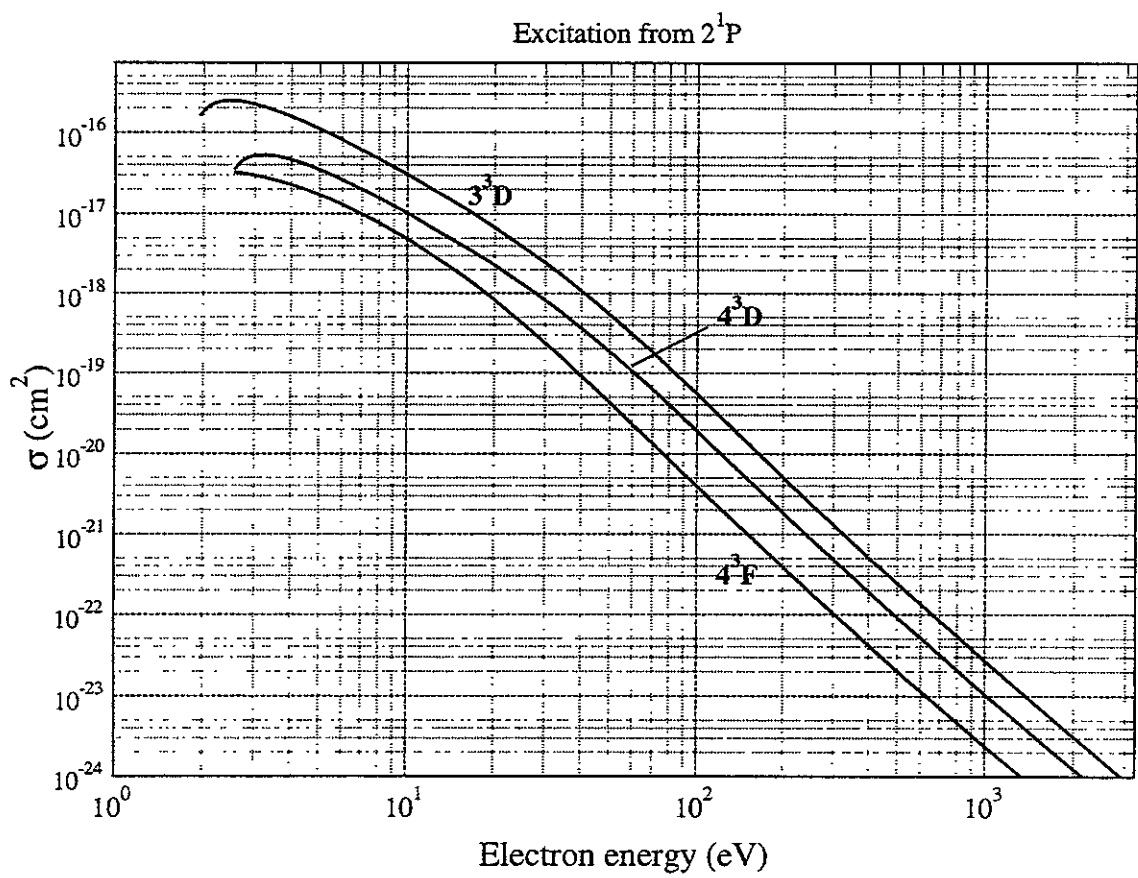
Graphs I 11



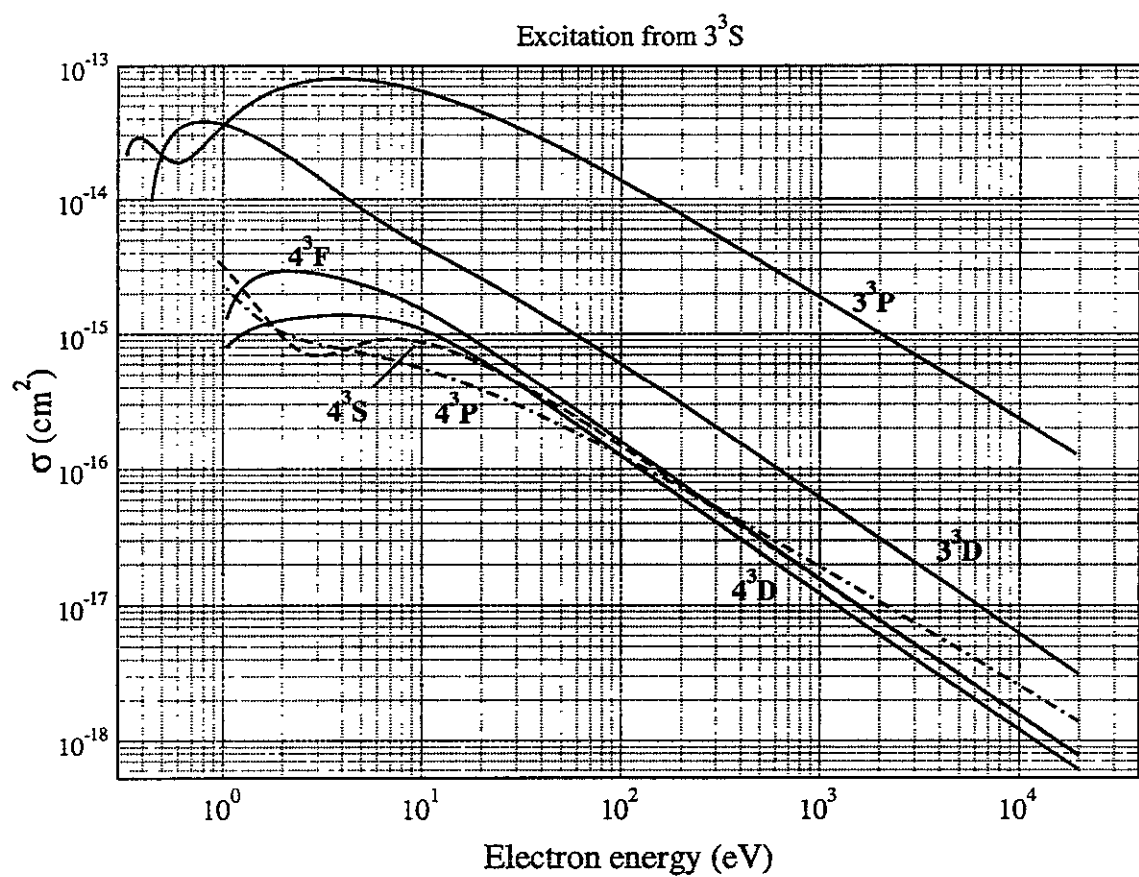
Graphs I 12



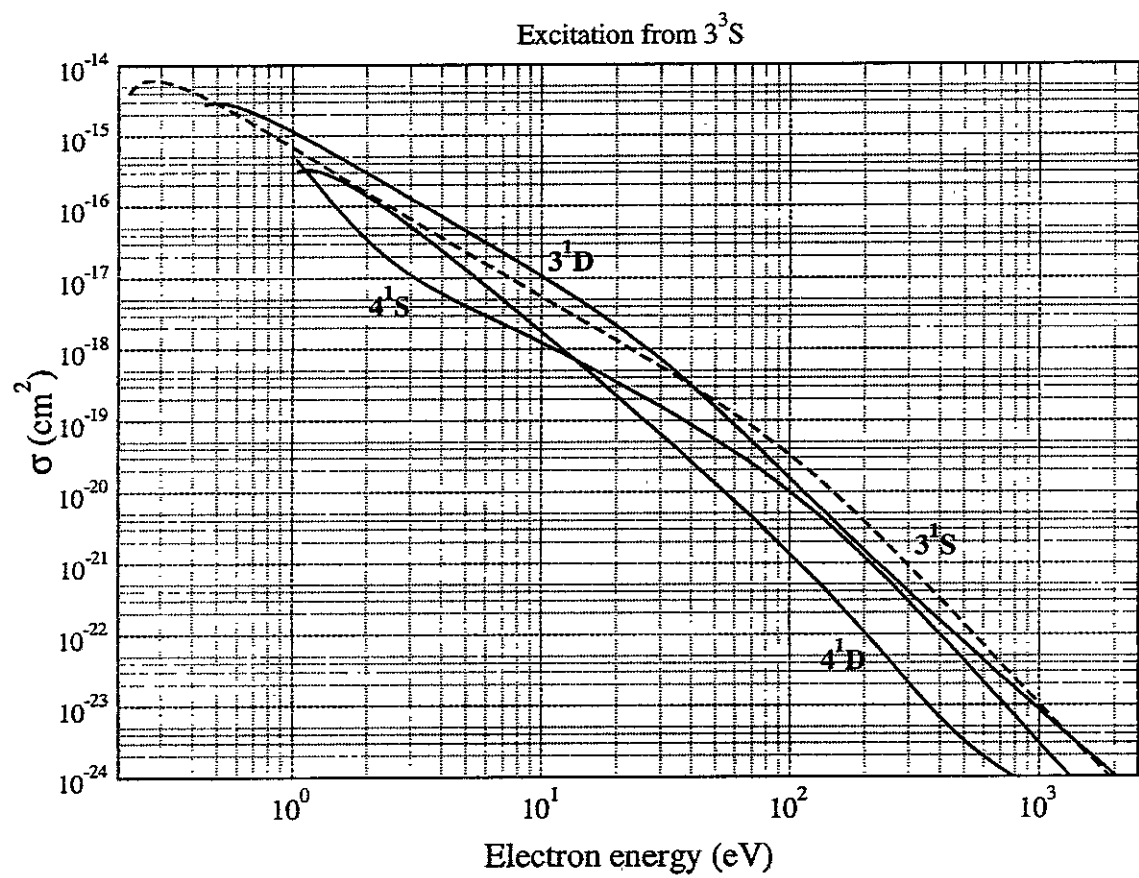
Graphs I 13



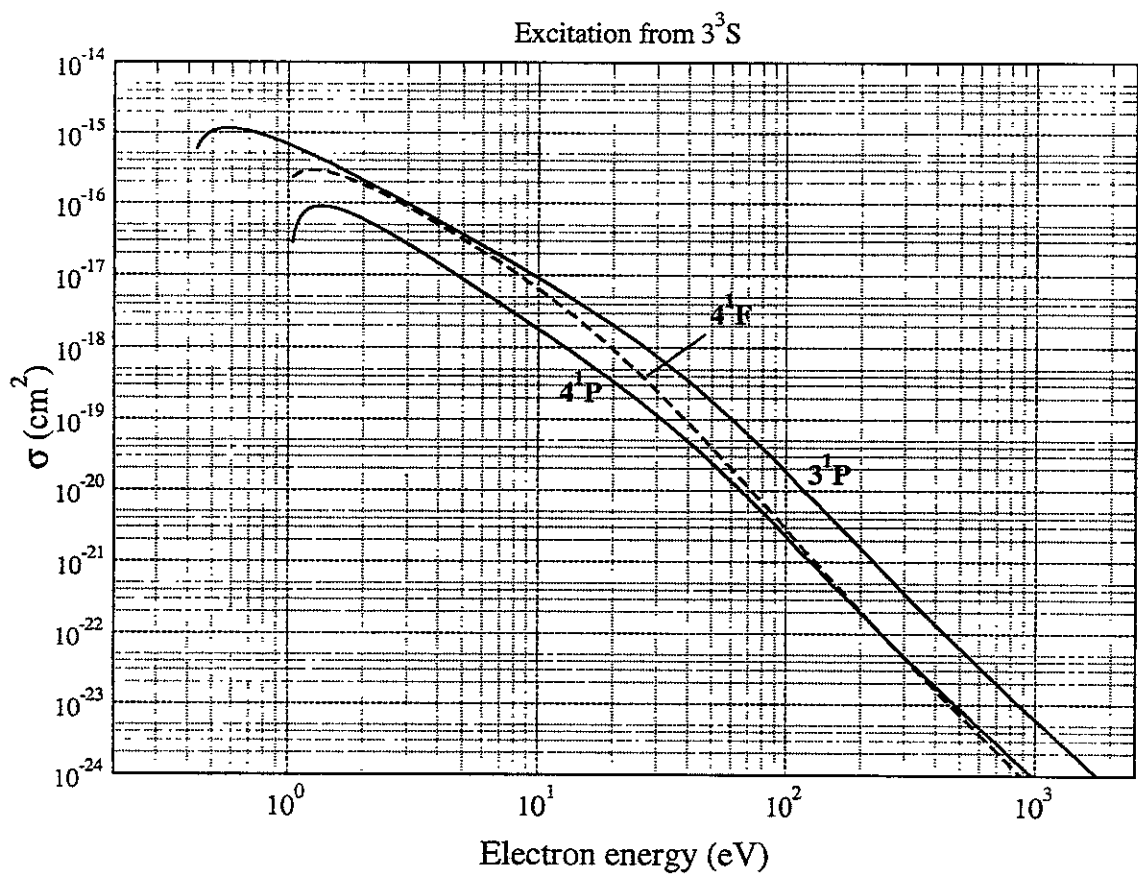
Graphs I 14



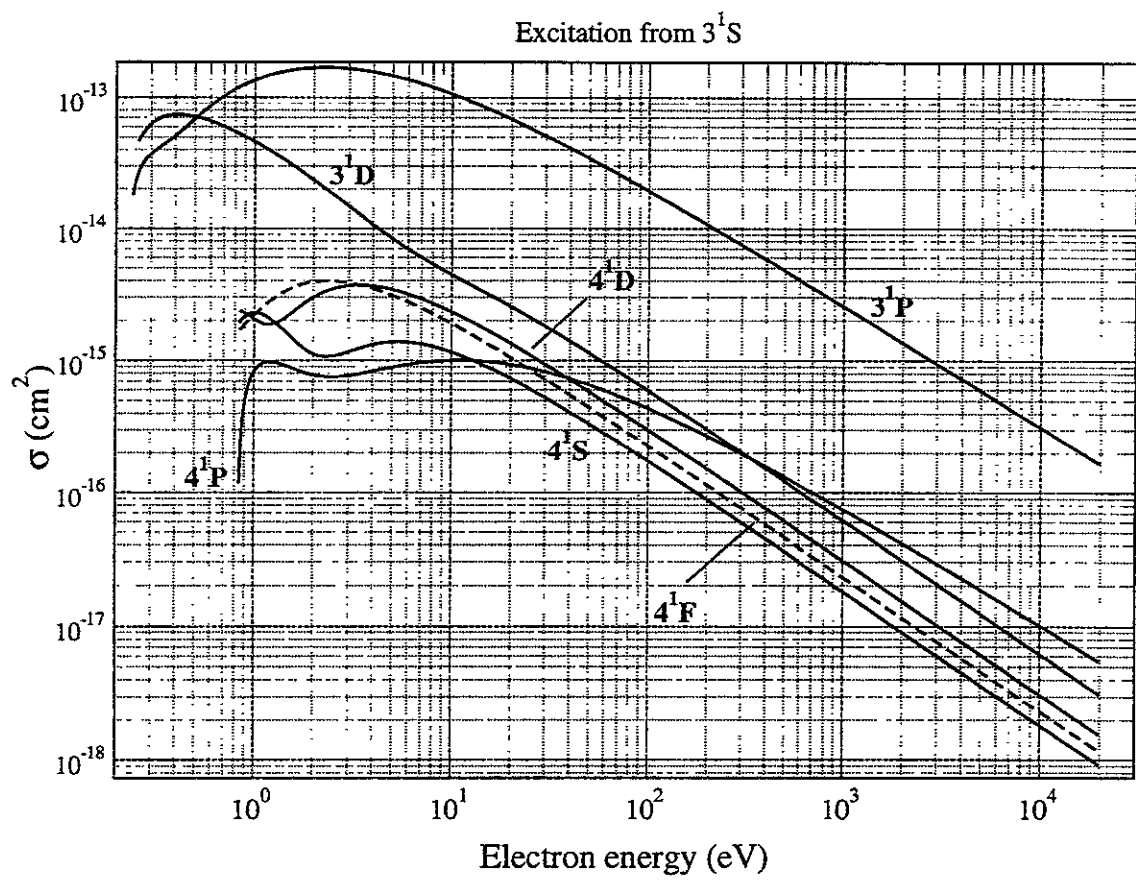
Graphs I 15



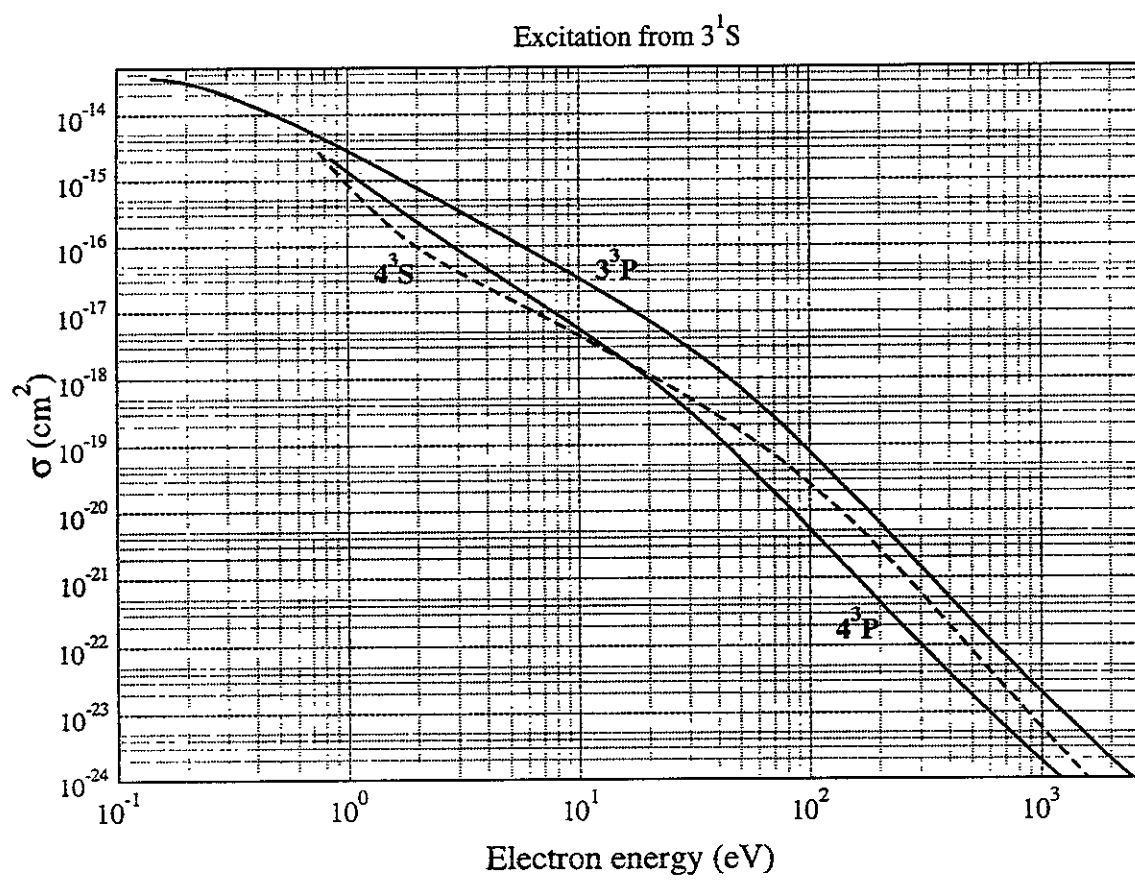
Graphs I 16



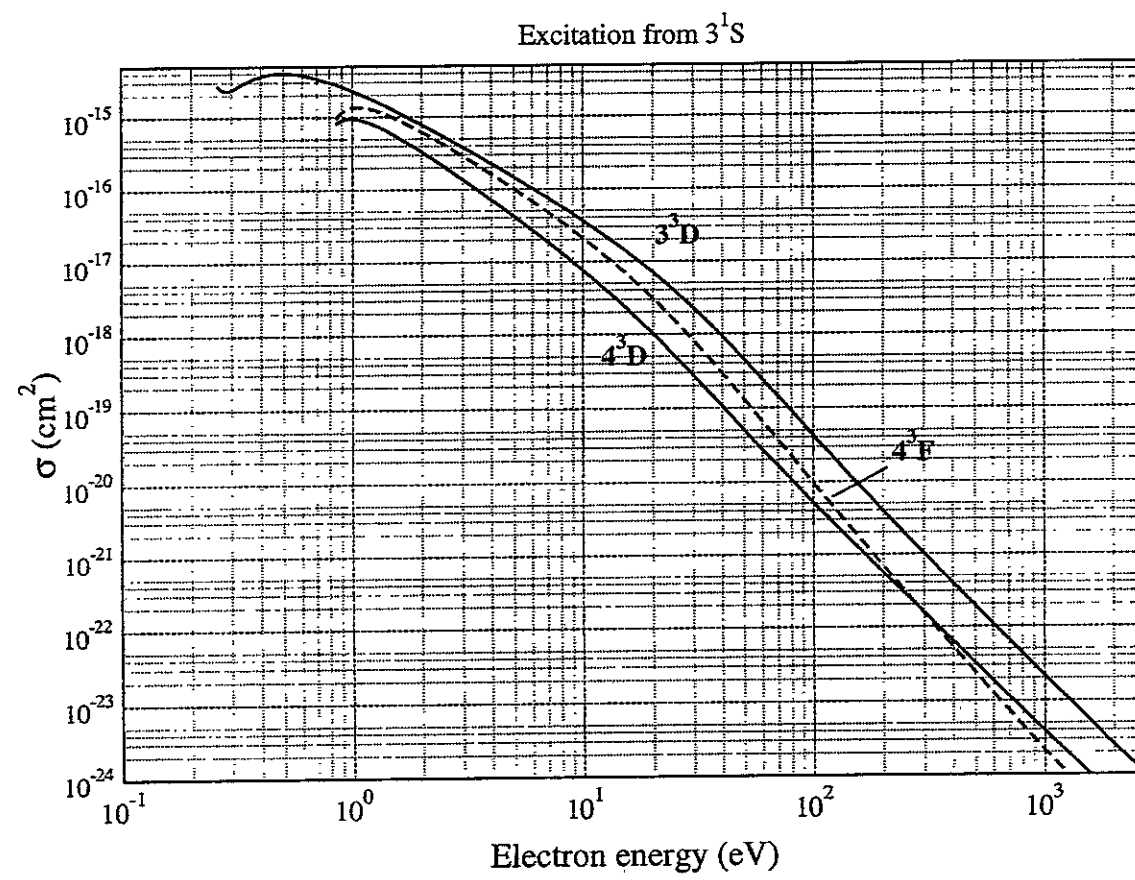
Graphs I 17



Graphs I 18

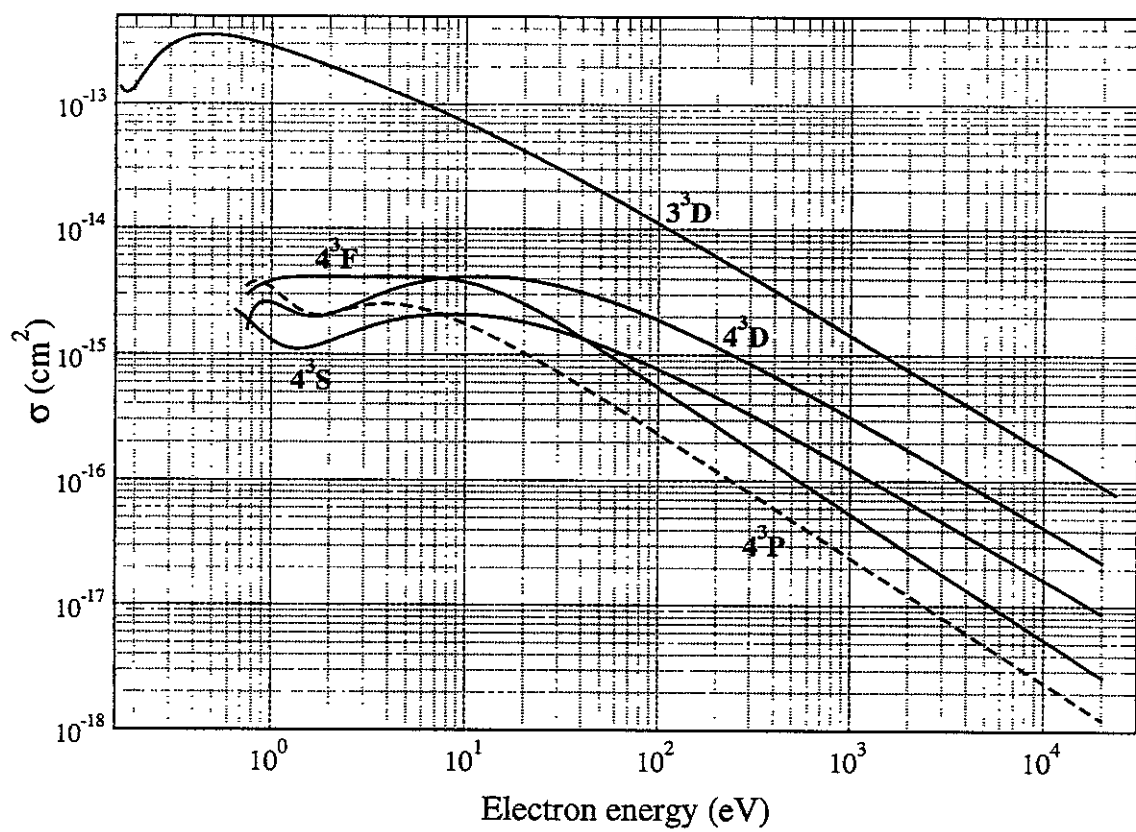


Graphs I 19



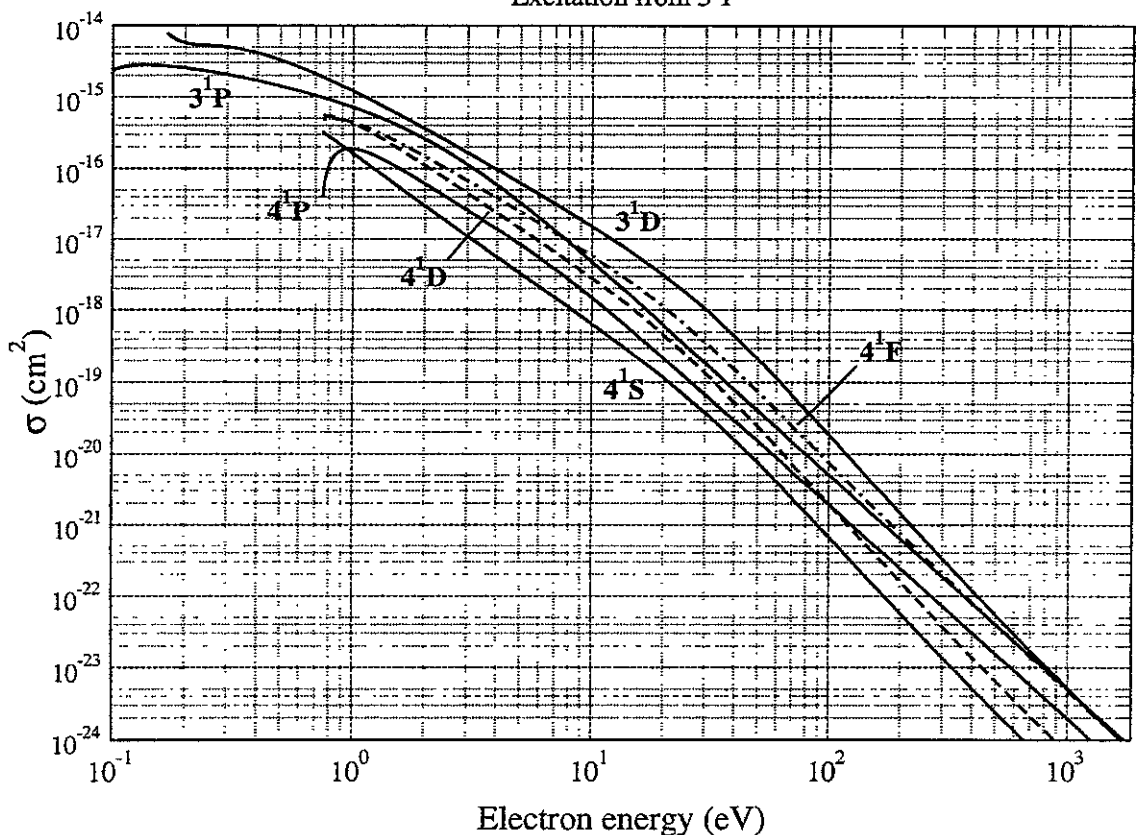
Graphs I 20

Excitation from  $3^3P$

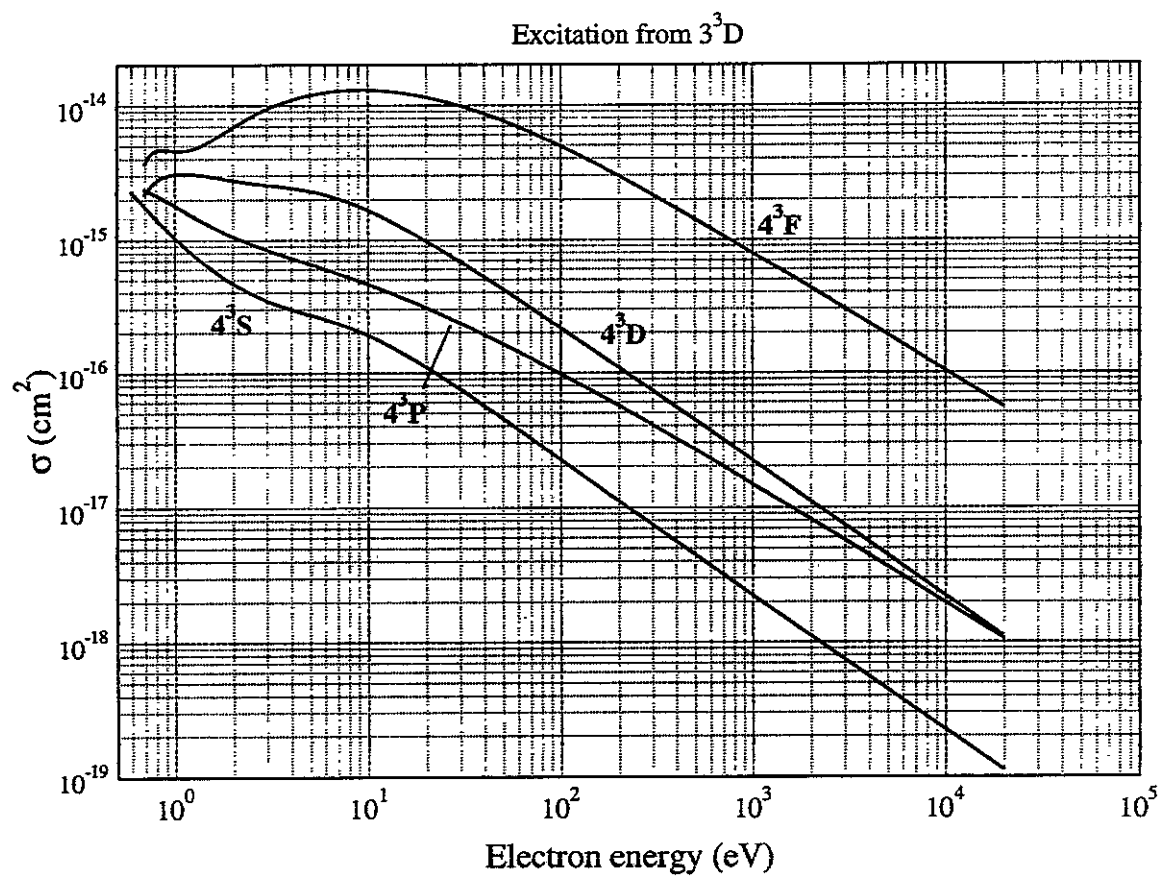


Graphs I 21

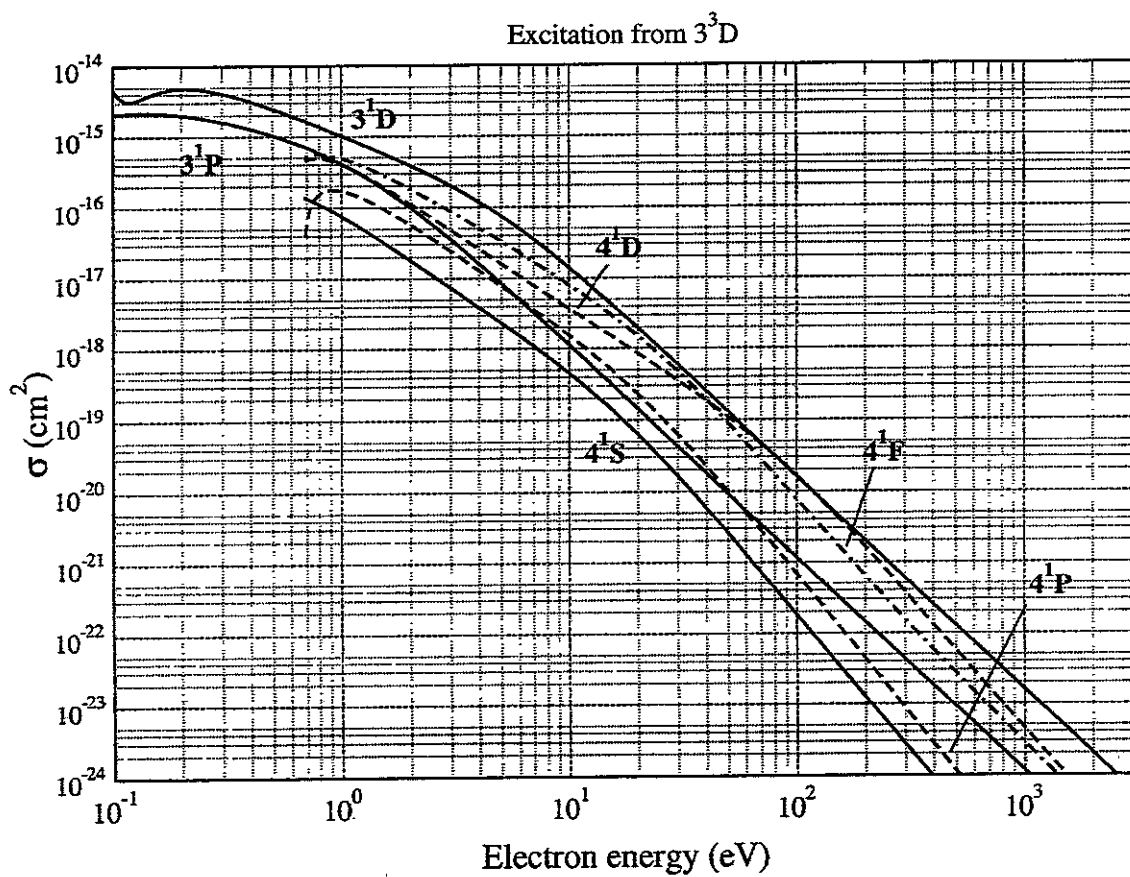
Excitation from  $3^3P$



Graphs I 22

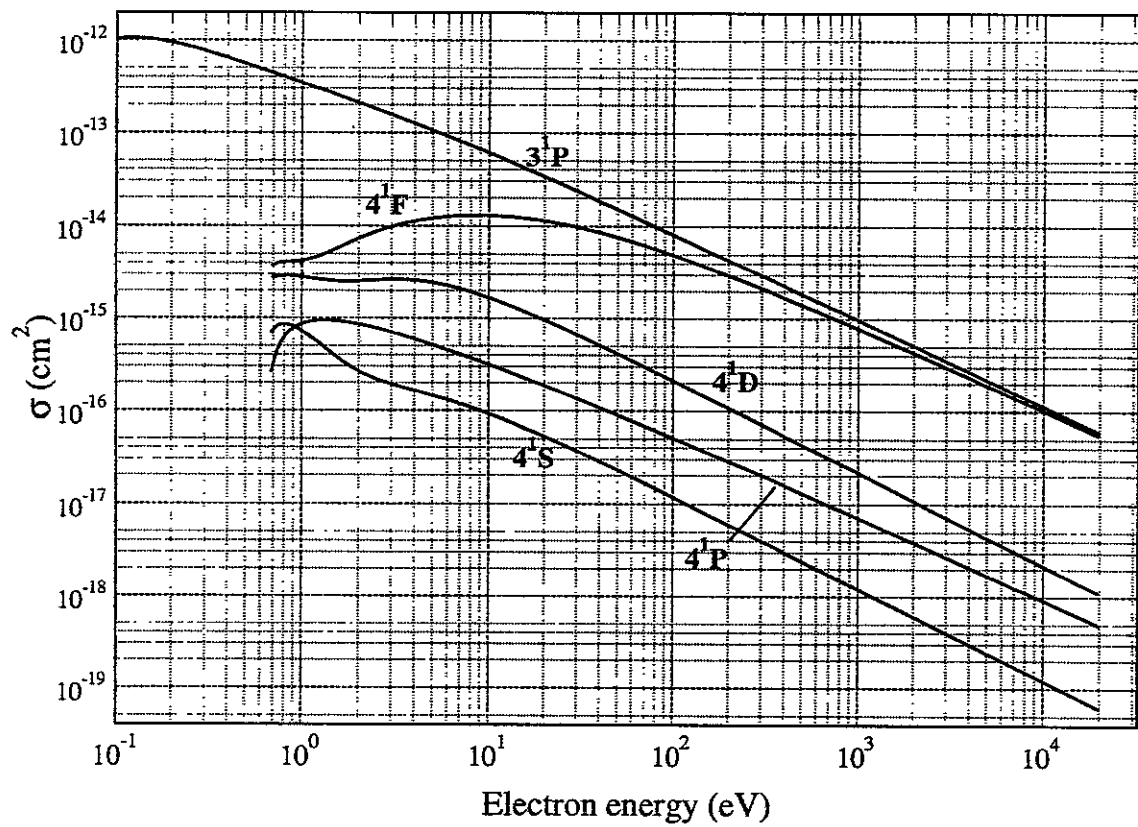


Graphs I 23



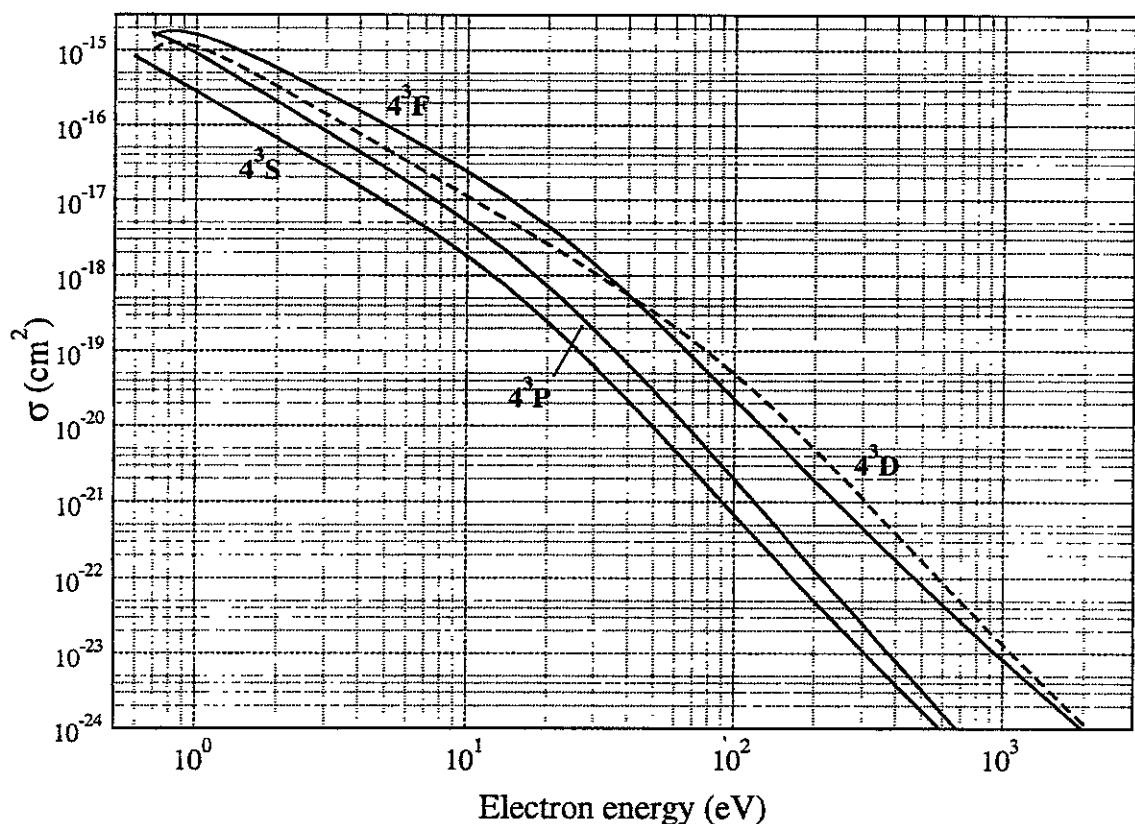
Graphs I 24

Excitation from  $3^1\text{D}$

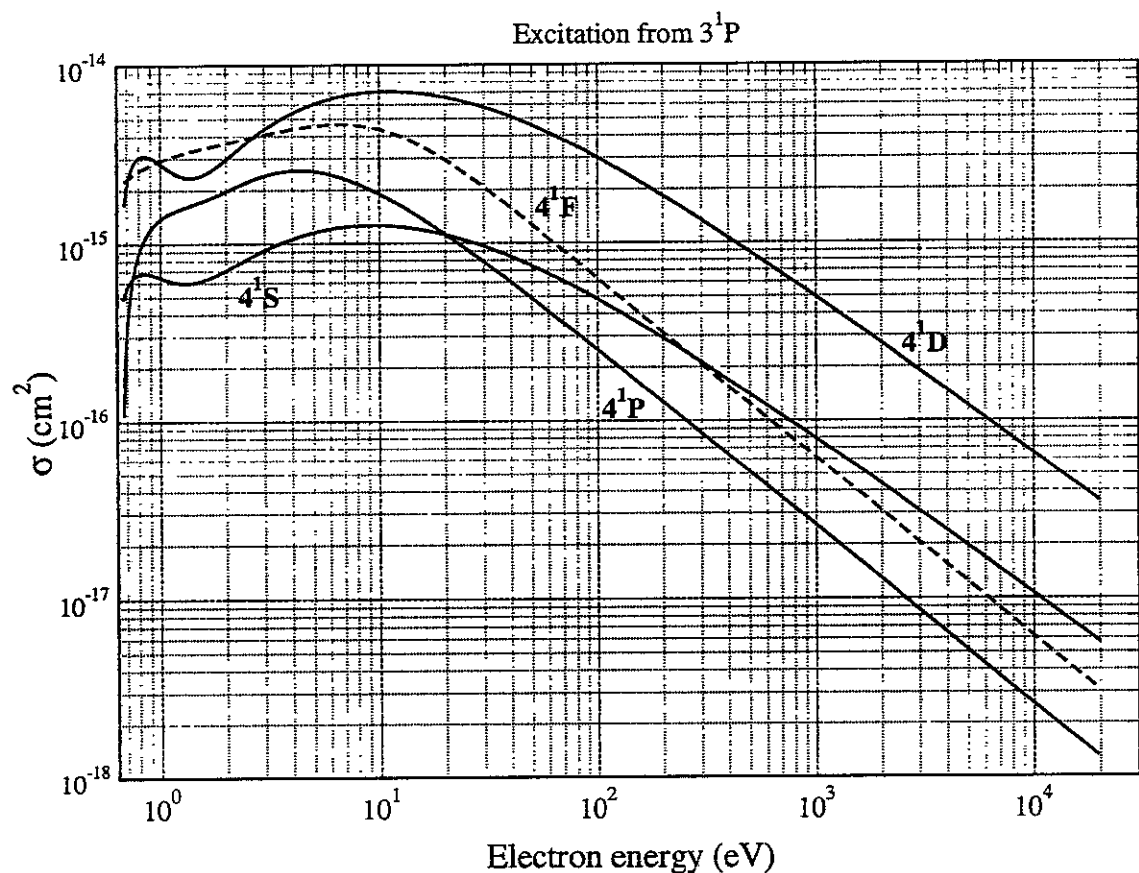


Graphs I 25

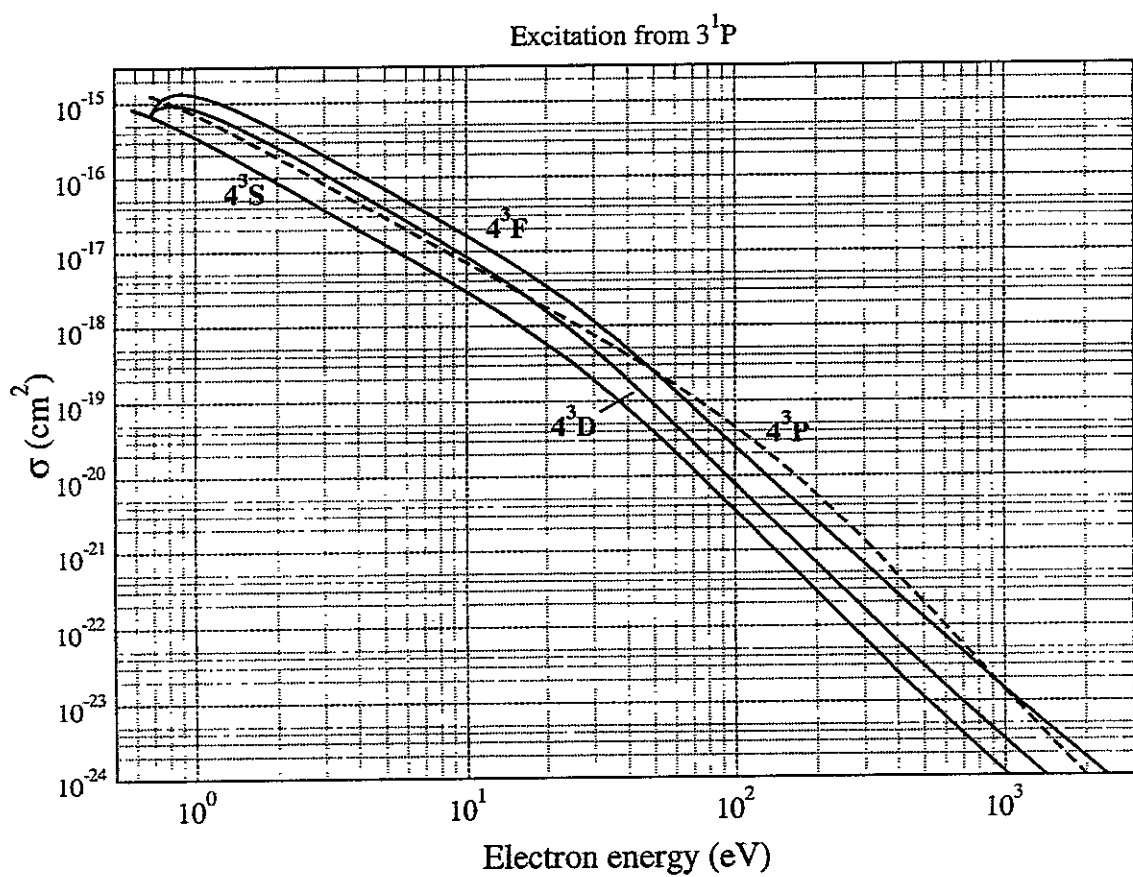
Excitation from  $3^1\text{D}$



Graphs I 26

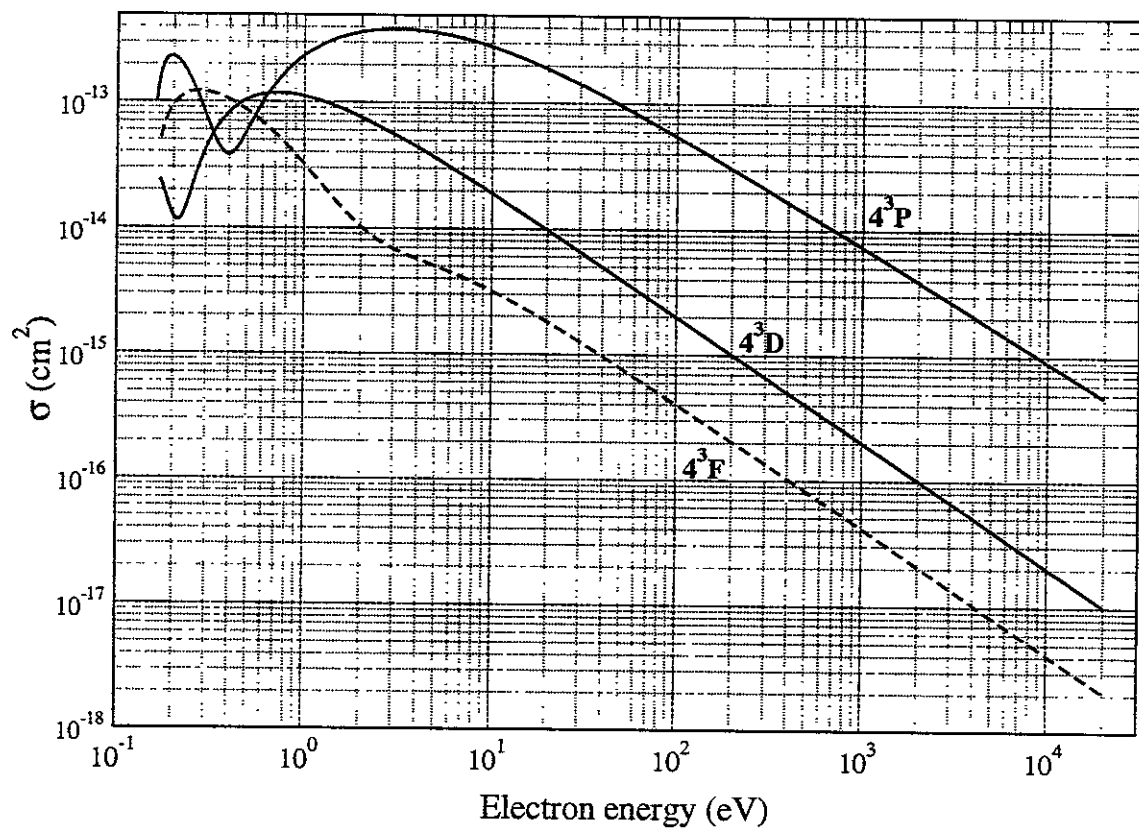


Graphs I 27



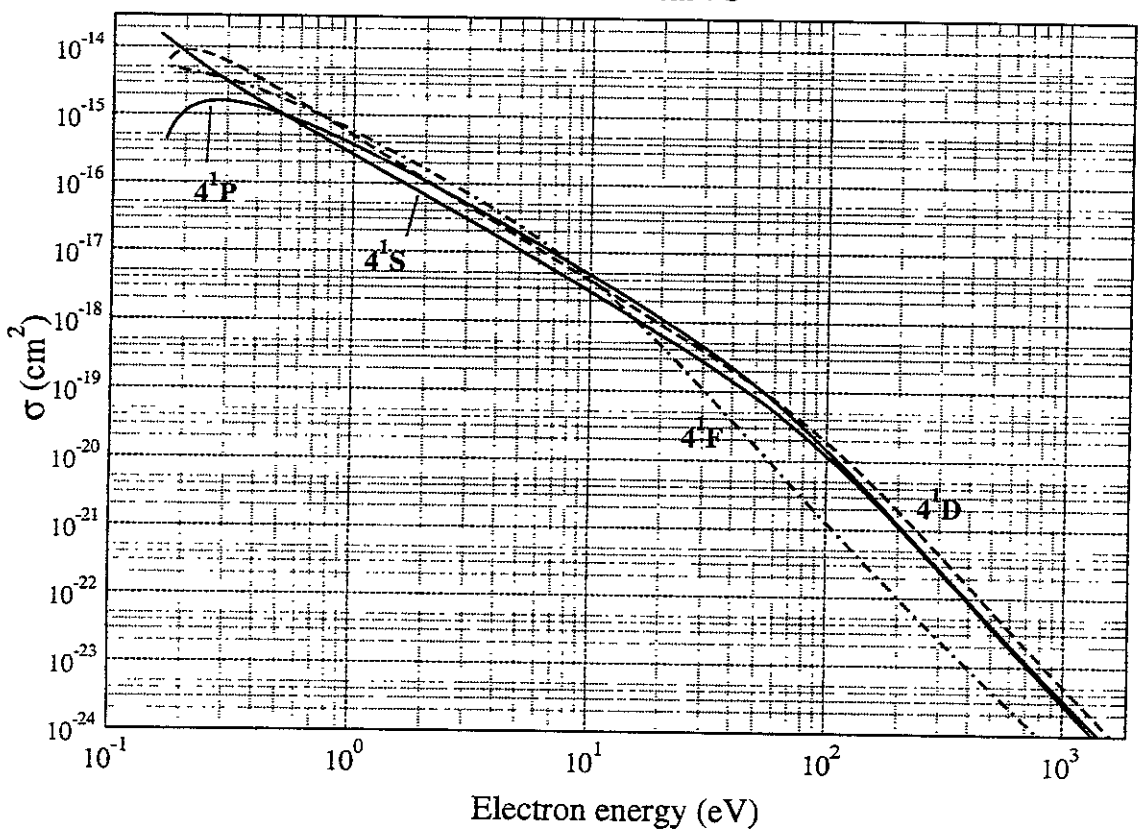
Graphs I 28

Excitation from  $4^3S$

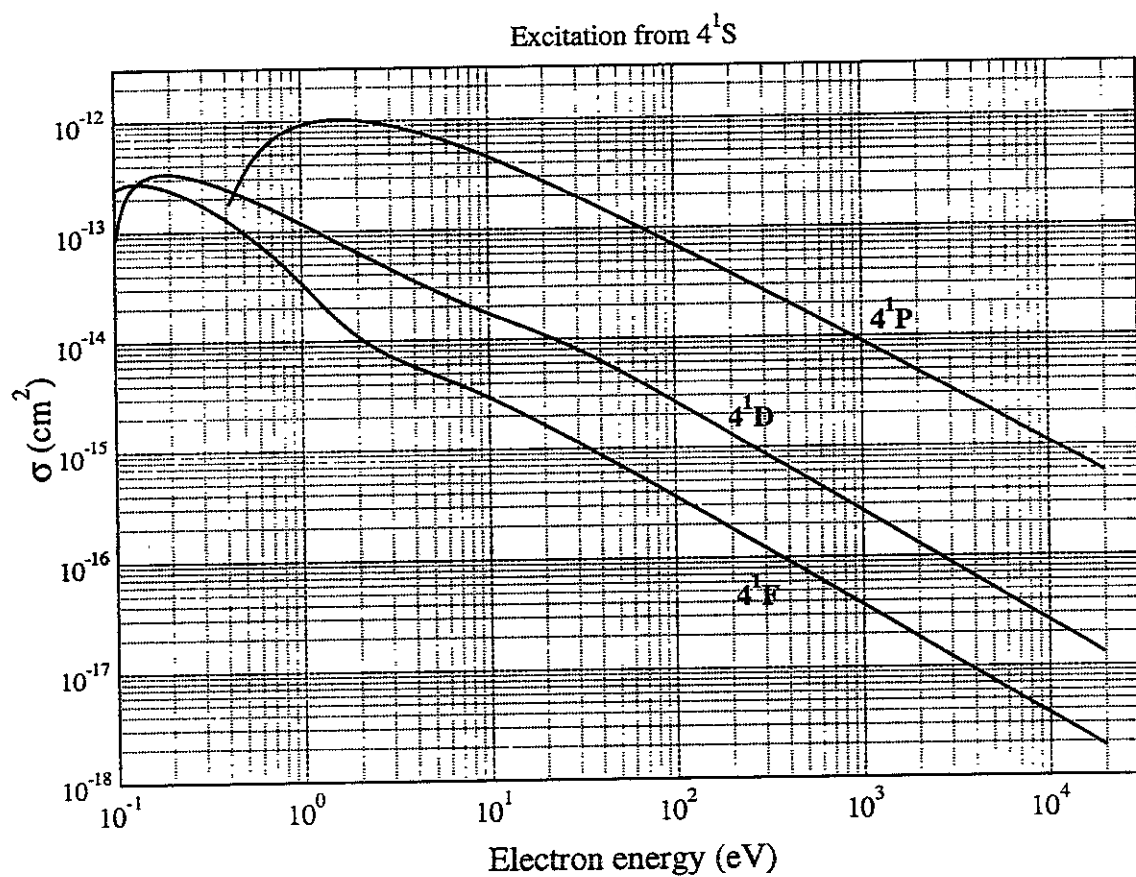


Graphs I 29

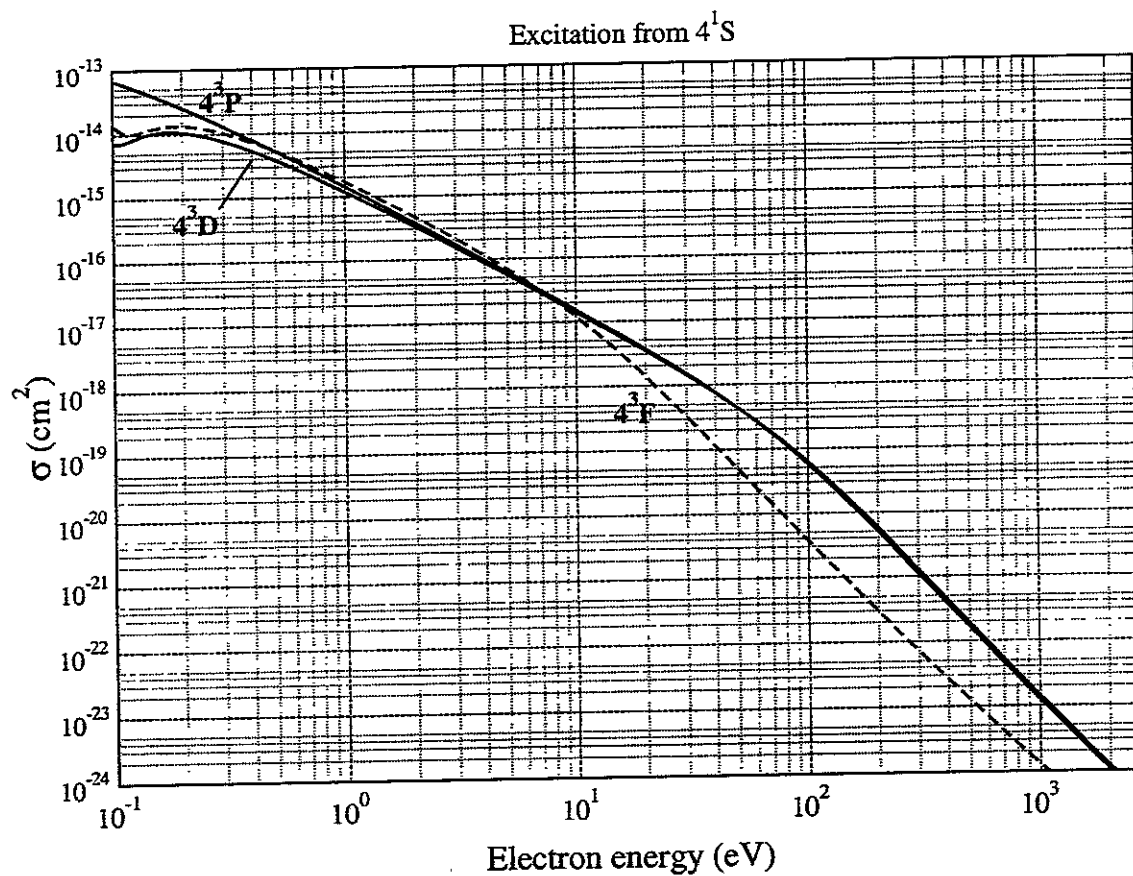
Excitation from  $4^3S$



Graphs I 30

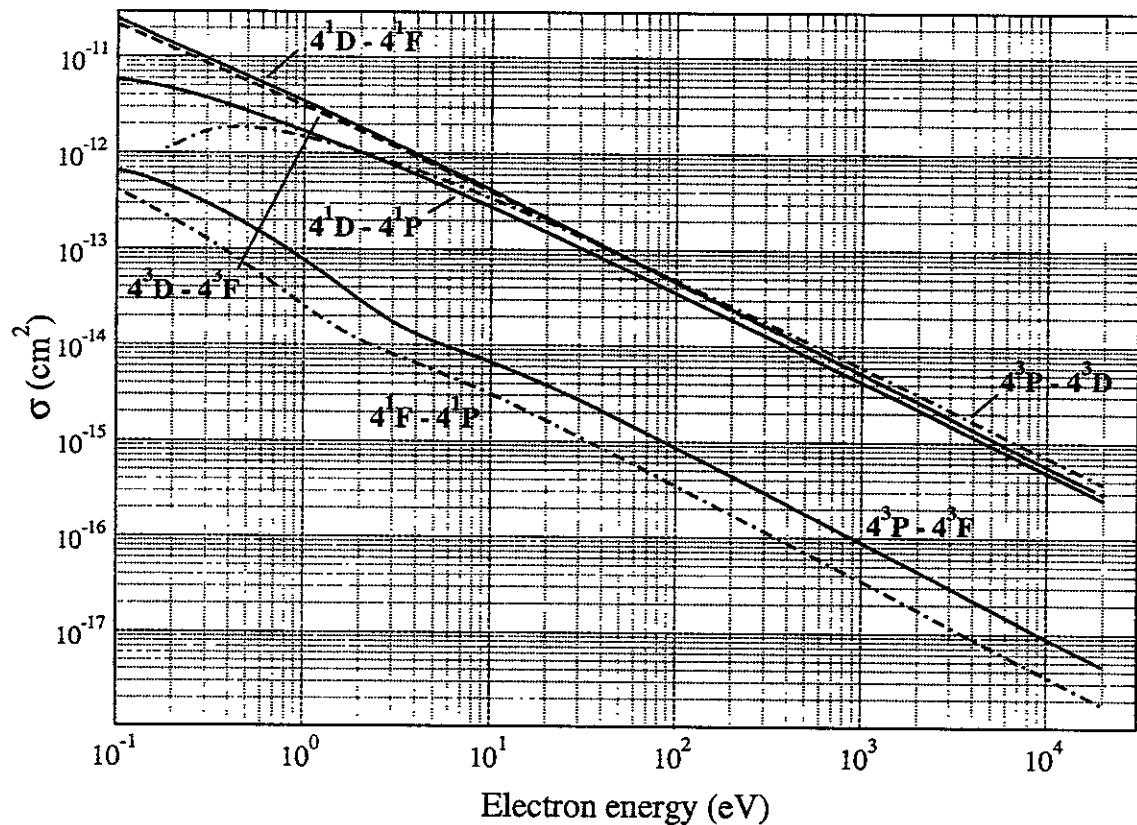


Graphs I 31

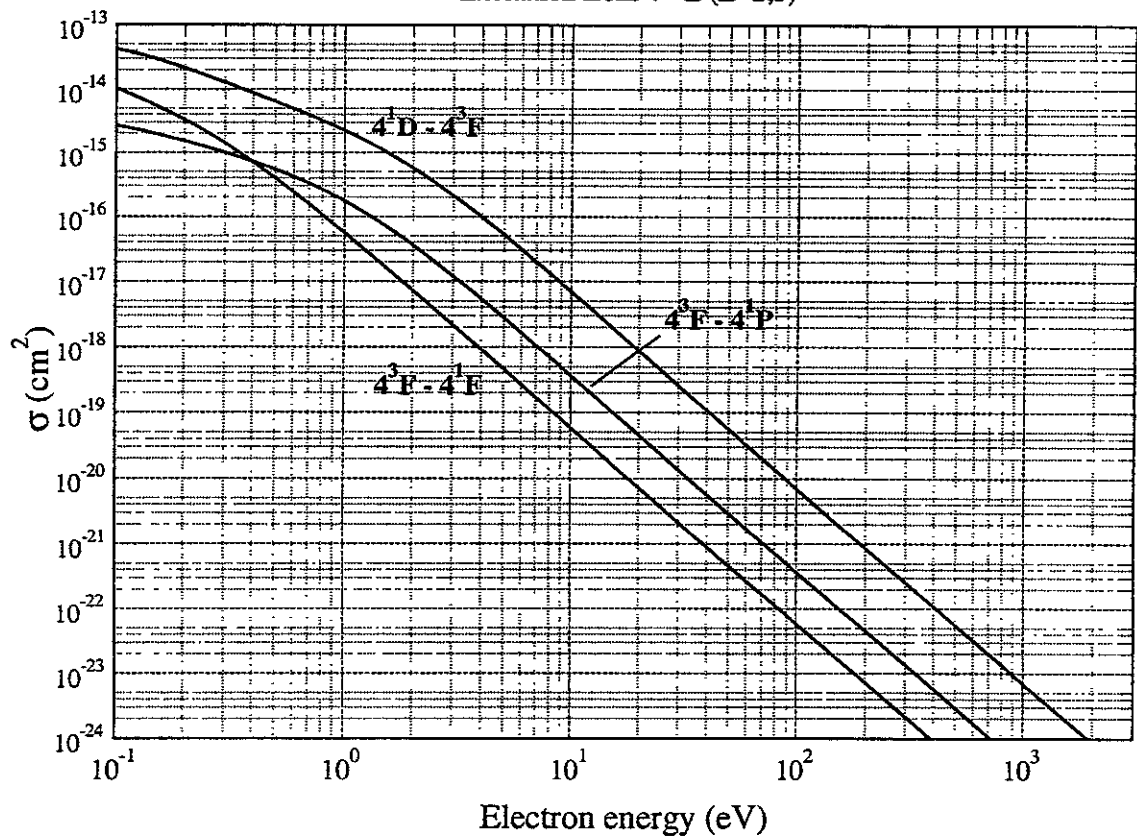


Graphs I 32

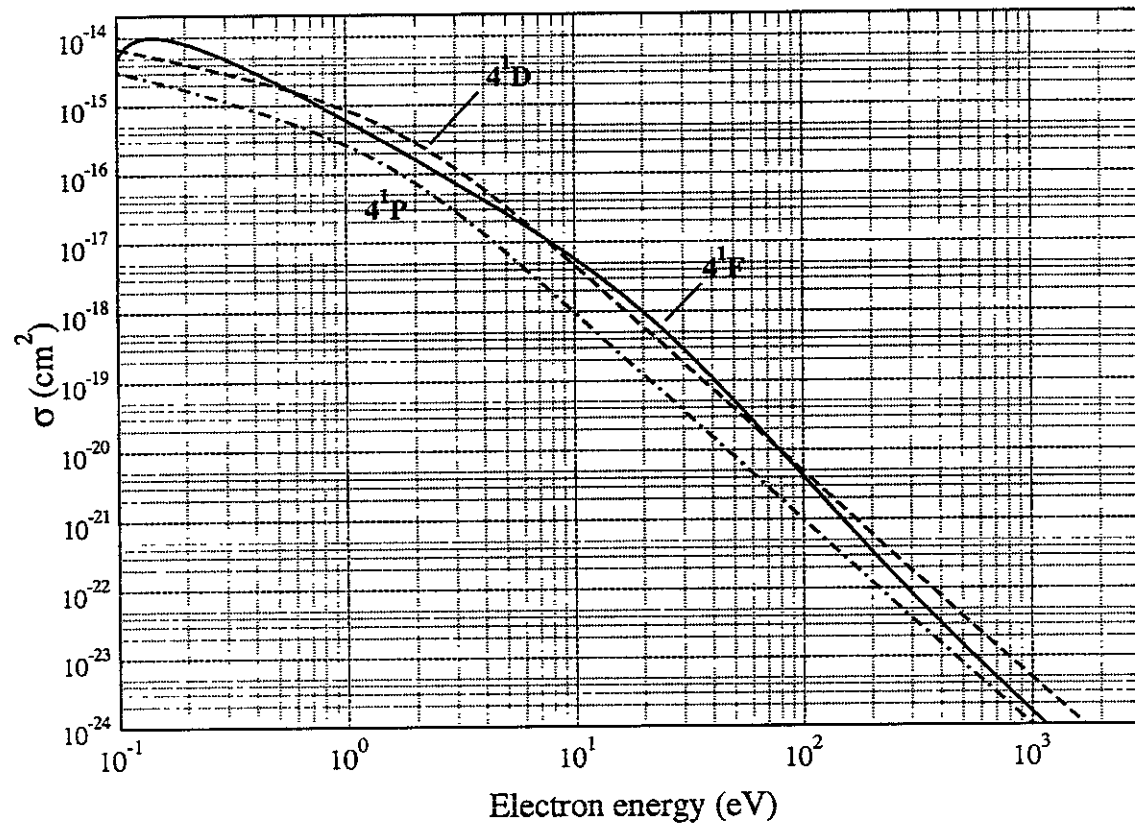
Excitation from  $4^{1,3}L$  ( $L>0$ )



Excitation from  $4^{1,3}L$  ( $L=2,3$ )

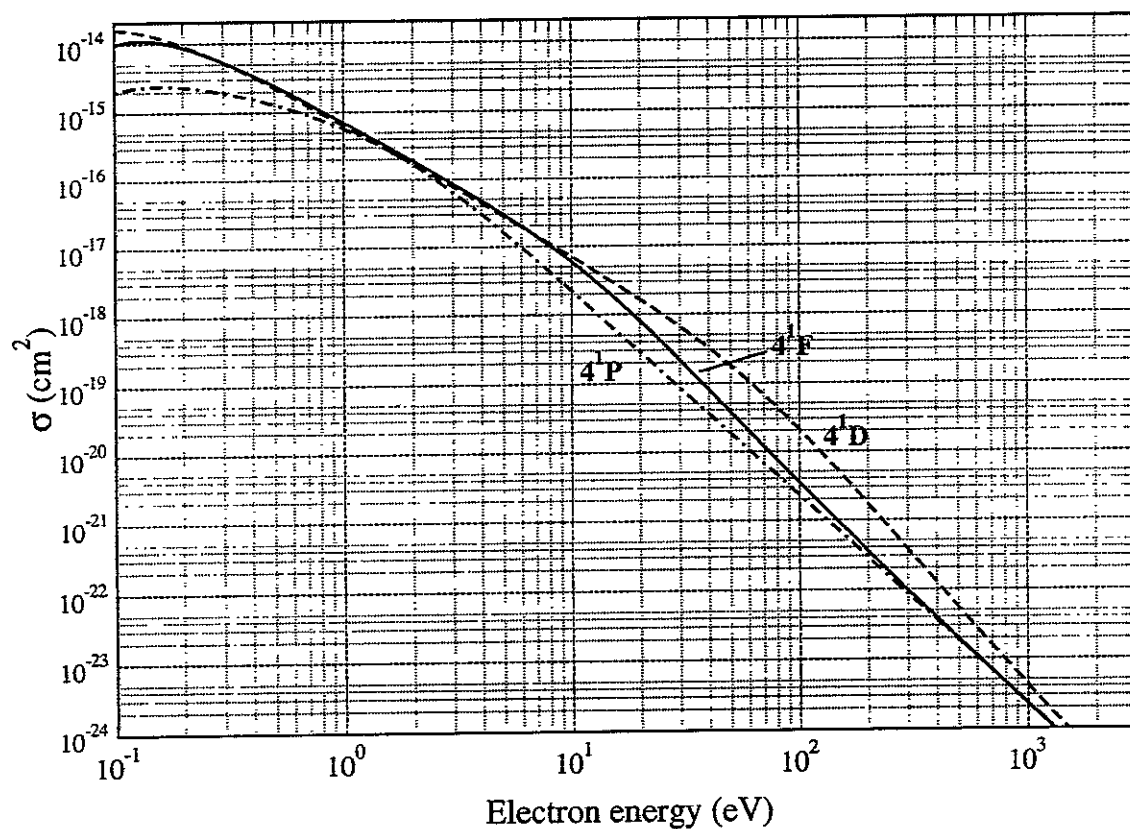


Excitation from  $4^3D$



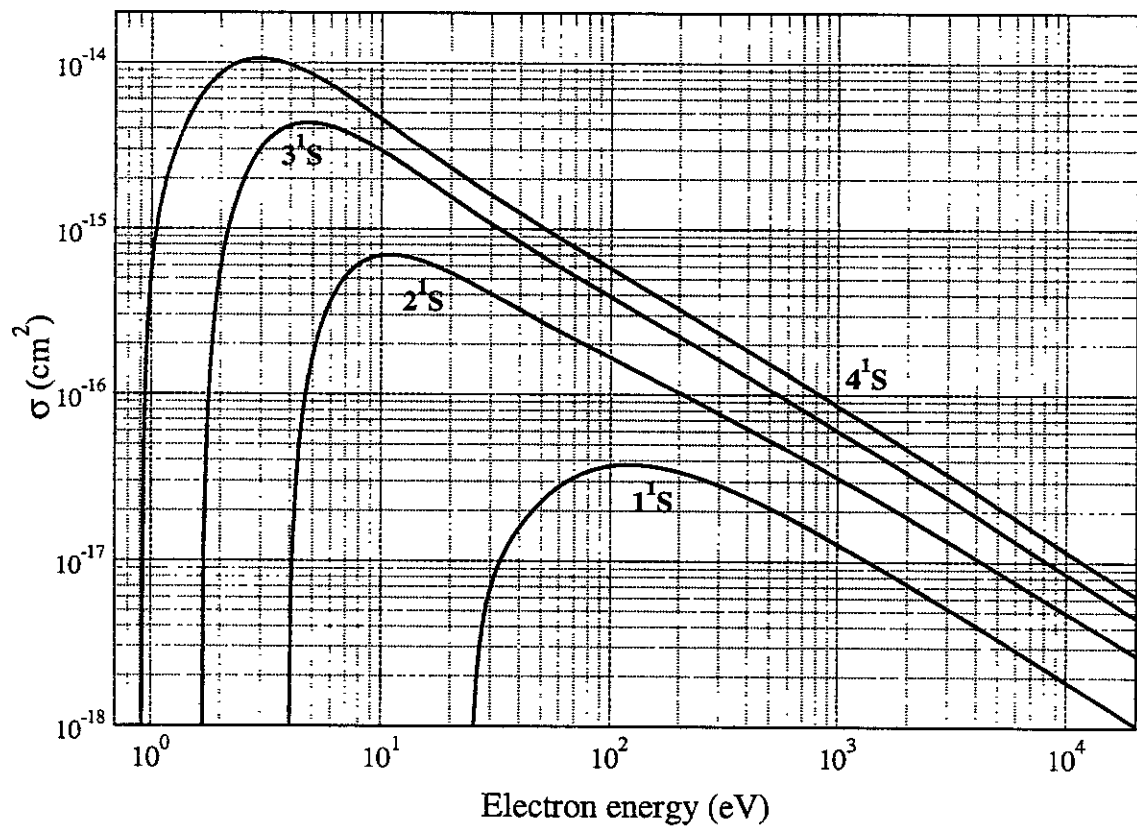
Graphs I 35

Excitation from  $4^3P$



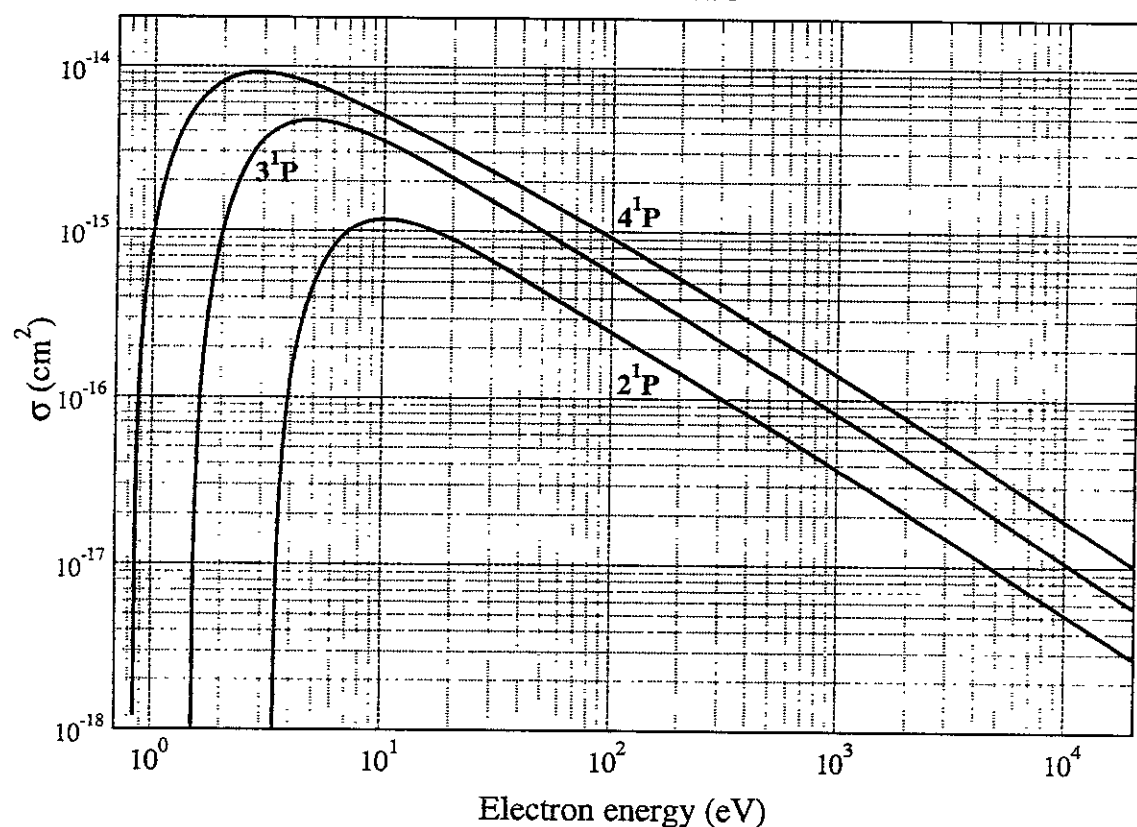
Graphs I 36

Ionization from  $n^1S$

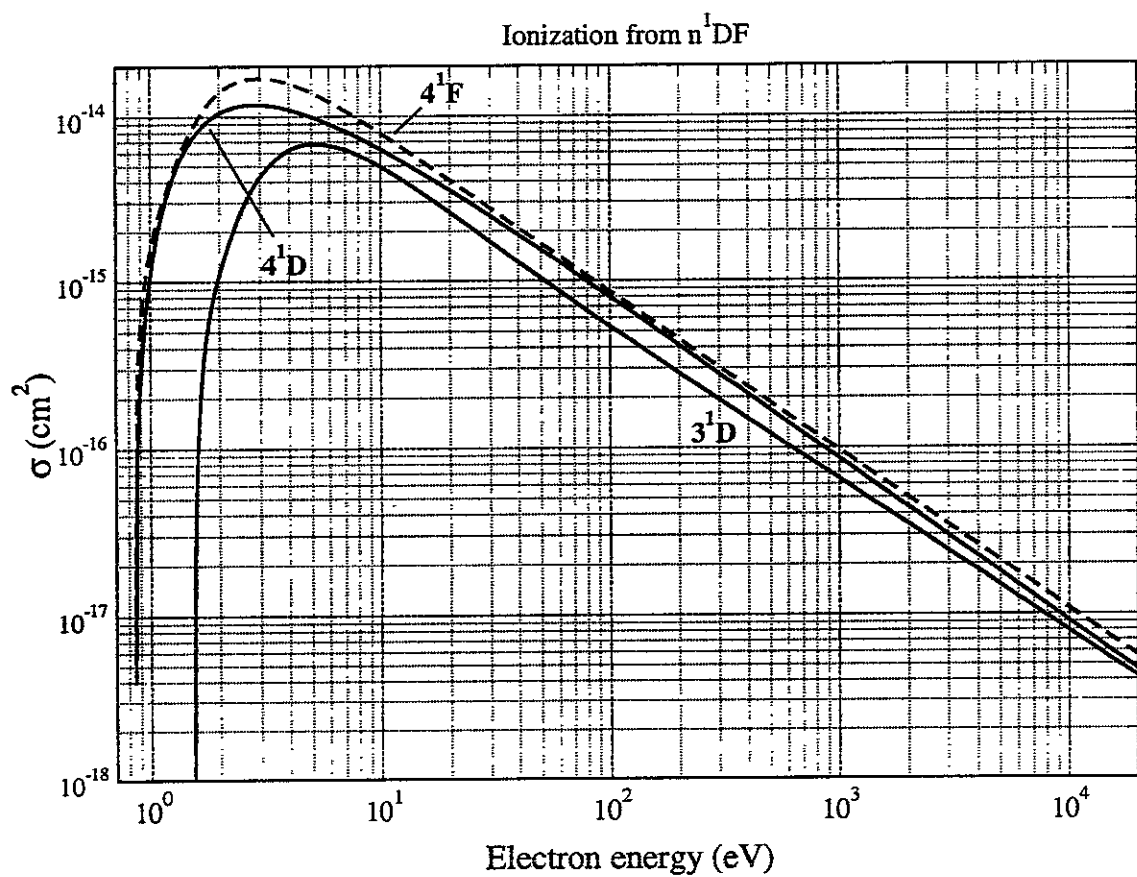


Graphs II 1

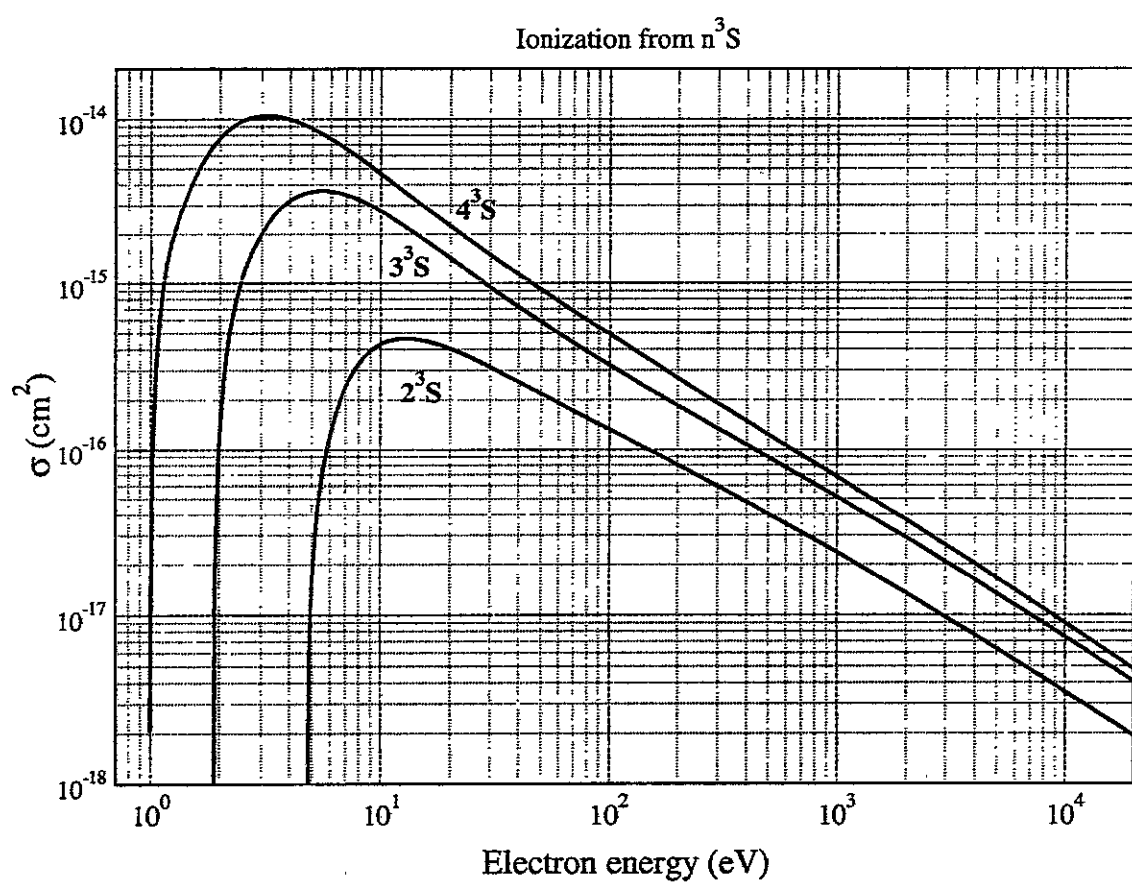
Ionization from  $n^1P$



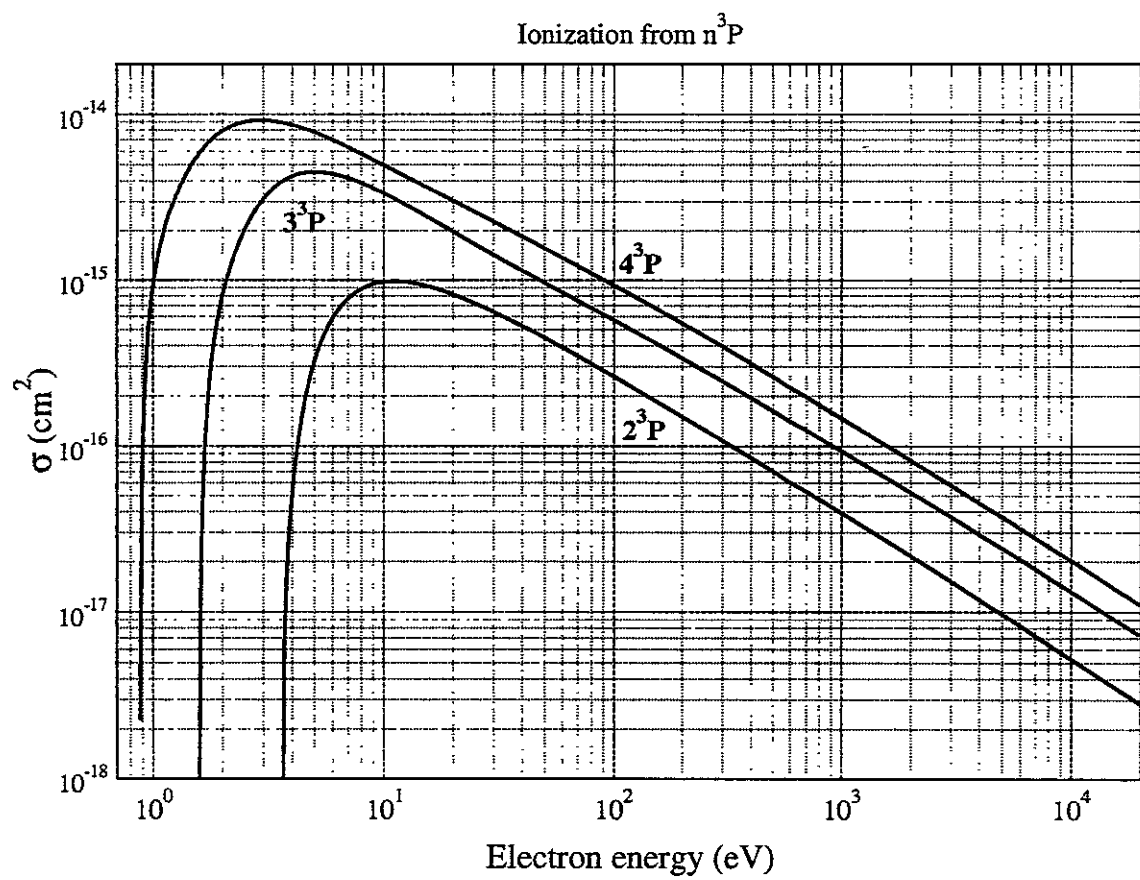
Graphs II 2



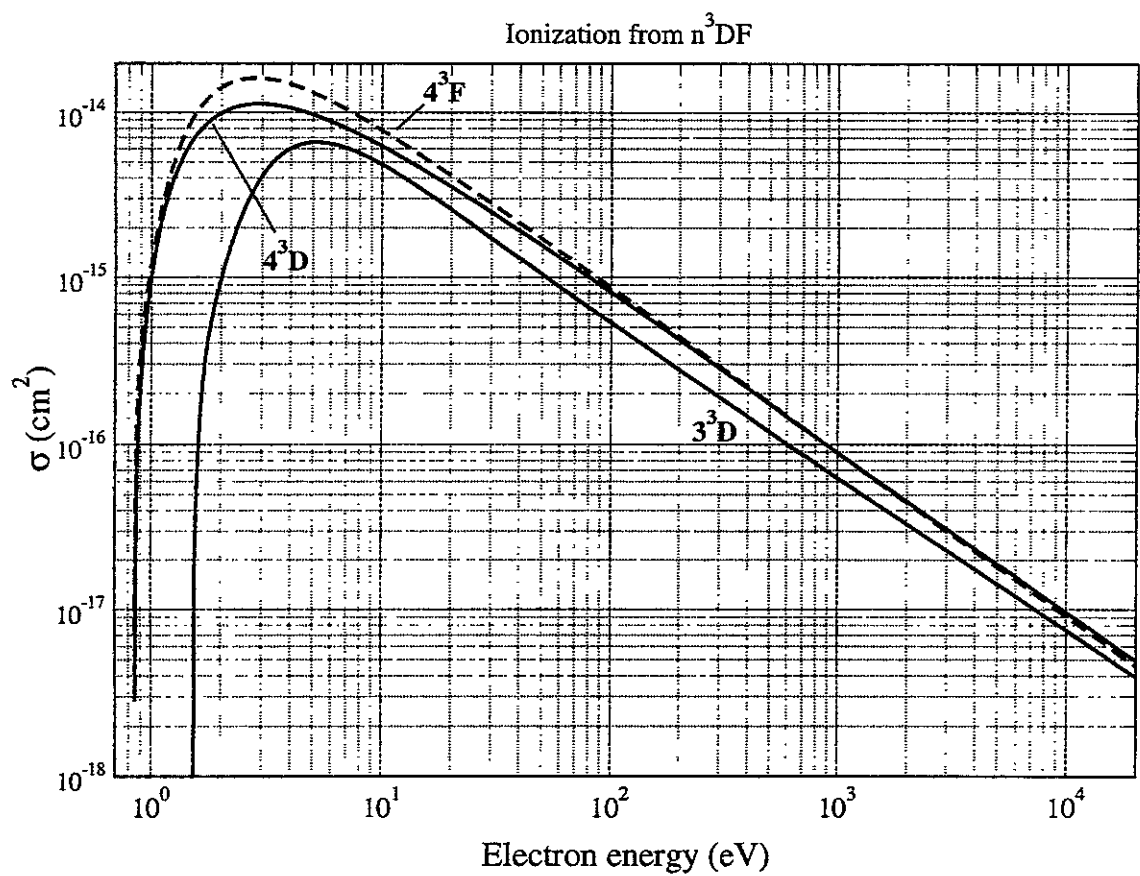
Graphs II 3



Graphs II 4



Graphs II 5



Graphs II 6

## Publication List of NIFS-DATA Series

- NIFS-DATA-43 M Goto and T Fujimoto,  
Collisional-radiative Model for Neutral Helium in Plasma: Excitation Cross Section and  
Singlet-triplet Wavefunction Mixing; Oct 1997
- NIFS-DATA-44 J Dubau, T. Kato and U.I Safronova,  
Dielectronic Recombination Rate Coefficients to the Excited States of CI From CII.Jan. 1998
- NIFS-DATA-45 Y Yamamura, W Takeuchi and T Kawamura,  
The Screening Length of Interatomic Potential in Atomic Collisions; Mar 1998
- NIFS-DATA-46 T Kenmotsu, T Kawamura, T Ono and Y. Yamamura,  
Dynamical Simulation for Sputtering of B4C; Mar 1998
- NIFS-DATA-47 I Murakami, K Moribayashi and T. Kato,  
Effect of Recombination Processes on FeXXIII Line Intensities; May 1998
- NIFS-DATA-48 Zhijie Li, T. Kenmotsu, T. Kawamura, T Ono and Y. Yamamura,  
Sputtering Yield Calculations Using an Interatomic Potential with the Shell Effect and a New  
Local Model; Oct. 1998
- NIFS-DATA-49 S. Sasaki, M. Goto, T. Kato and S.Takamura,  
Line Intensity Ratios of Helium Atom in an Ionizing Plasma;Oct 1998
- NIFS-DATA-50 I Murakami, T Kato and U. Safronova,  
Spectral Line Intensities of NeVII for Non-equilibrium Ionization Plasma Including  
Dielectronic Recombination Processses, Jan. 1999
- NIFS-DATA-51 Hiro Tawara and Masa Kato,  
Electron Impact Ionization Data for Atoms and Ions -up-dated in 1998-,Feb 1999
- NIFS-DATA-52 J.G. Wang, T. Kato and I. Murakami,  
Validity of  $n^{-3}$  Scaling Law in Dielectronic Recombination Processes; Apr. 1999
- NIFS-DATA-53 J.G. Wang, T. Kato and I. Murakami,  
Dielectronic Recombination Rate Coefficients to Excited States of He from  $\text{He}^+$ , Apr. 1999
- NIFS-DATA-54 T Kato and E. Asano,  
Comparison of Recombination Rate Coefficients Given by Empirical Formulas for Ions from  
Hydrogen through Nickel; June 1999
- NIFS-DATA-55 H.P Summers, H Anderson, T. Kato and S Murakami,  
Hydrogen Beam Stopping and Beam Emission Data for LHD,Nov. 1999
- NIFS-DATA-56 S. Born, N. Matsunari and H Tawara,  
A Simple Theoretical Approach to Determine Relative Ion Yield (RIY) in Glow Discharge Mass  
Spectrometry (GDMS),Jan 2000
- NIFS-DATA-57 T Ono, T Kawamura, T Kenmotsu, Y. Yamamura,  
Simulation Study on Retention and Reflection from Tungsten Carbide under High Fluence of  
Helium Ions; Aug. 2000
- NIFS-DATA-58 J.G Wang, M. Kato and T. Kato,  
Spectra of Neutral Carbon for Plasma Diagnostics; Oct 2000
- NIFS-DATA-59 Yu. V. Ralchenko, R. K. Janev, T. Kato, D.V Fursa, I. Bray and F.J de Heer  
Cross Section Database for Collision Processes of Helium Atom with Charged Particles.  
I. Electron Impact Processes; Oct. 2000